NATIONAL ADVISORY COMMITTEE FOR AERONAUTICS

TECHNICAL NOTE 2830

SEVERAL COMBINATION PROBES FOR SURVEYING STATIC AND TOTAL PRESSURE AND FLOW DIRECTION

By Wallace M. Schulze, George C. Ashby, Jr., and John R. Erwin

Langley Aeronautical Laboratory
Langley Field, Va.

Washington
November 1952

NATIONAL ADVISORY COMMITTEE FOR AERONAUTICS

TECHNICAL NOTE 2830

SEVERAL COMBINATION PROBES FOR SURVEYING STATIC AND TOTAL PRESSURE AND FLOW DIRECTION

By Wallace M. Schulze, George C. Ashby, Jr., and John R. Erwin

SUMMARY

An investigation has been conducted to provide a basis for the design of combination probes intended to survey the static and total pressure and direction of flow with special reference to subsonic turbomachine testing. Static-pressure probes, yaw-element probes, claw-type yaw probes, and combination probes were tested in an 8-inch-diameter calibration tunnel at air velocities up to 445 feet per second.

From the results of this investigation, the factors which determine the sensitivity of claw-type yaw probes were determined. Satisfactory combination survey probes for sensing static and total pressure and direction of flow in one or two planes were devised.

INTRODUCTION

The accurate measurement of flow properties is required throughout the field of aerodynamic testing. When the flow under study is contained within small passages or when the flow properties change significantly within a short distance, as in turbomachines, the probes used to survey the flow can affect the results. The probe indications may be affected by local alteration of the flow because of the presence of the probe, by the inability of the probe to take all readings simultaneously at a point, by changes in calibration factors resulting from Reynolds number or Mach number effects, or by probe deformation. In order to minimize the errors due to these sources, a combination probe for subsonic turbomachine testing must be very small, capable of point measurement, adaptable to many uses and wide speed ranges, and suitable for use in the presence of small cross flows; the probe should also have a high flow-angle-indication sensitivity, negligible static- and total-pressure correction factors, rapid response, rugged construction, and a calibration insensitive to small construction irregularities. A combination flow-surveying probe having these properties has been

needed for use in several research programs, and the present investigation was inaugurated to provide an acceptable design of a combination probe for these programs.

A review of many reports has indicated that the simplest and most reliable methods of measuring the desired quantities individually have been standardized. The total pressure is conveniently indicated with an open tube pointed directly into the flow. References 1 and 2 present the results of an extensive study of total-pressure probes. Reference 1 concludes in part that the best results are obtained if the impact opening is as large as the tube will allow. No further study of this subject was considered necessary for the present investigation.

The static pressure is usually indicated with a round-end tube having small orifice openings placed several tube diameters downstream of the tip. A study of seven static-pressure probes is presented in reference 3. This work, however, was done at low speeds; therefore, certain phases of this study were repeated and the scope extended in the present investigation. Reference 4 presents the distribution of static pressure along tubes having several types of heads and indicates that a static-pressure error of less than 1 percent of the dynamic pressure may be expected at small tube attitudes if the static orifices are 3 or more probe diameters downstream of the base of the nose. In reference 5, the effect of orifice size on static-pressure indication was investigated in tests of long cylindrical probes 0.39 to 1.59 inches in diameter. This paper concludes that the ratio of orifice depth to orifice diameter can be varied from approximately 4 to 0.1 and the ratio of orifice diameter to probe diameter can be varied from approximately 0.01 to 0.5 without a significant change in static-pressure indication. Since the present investigation was concerned with short probes of small diameter and reference 5 did not state a definite Reynolds number range, a study of 0.060-inch-, 0.125-inch-, and 0.25-inch-diameter probes was made over a Reynolds number range (based on probe diameter) of 3,000 to 53,000. The ratio of orifice depth to orifice diameter was varied from 1.67 to 0.5 and the ratio of orifice diameter to probe diameter was varied from 0.04 to 0.33 without an appreciable change in static-pressure indication. These values were followed in the design of all probes for this report.

A common method of obtaining flow direction is the null system, which makes use of a probe consisting of two symmetrically mounted open-end tubes with the faces of the open ends making equal and opposite angles with the air stream. The probe is rotated until both tubes indicate equal pressures. A properly designed and constructed null-type probe should not be affected by changes in Reynolds number or Mach number. The null system is well-suited to the design of combination surveying probes, since static and total pressure can be measured most accurately when the probe is alined with the air stream. Yaw probes of this type usually require calibration in a known air flow and are somewhat

inaccurate in flow fields containing total-pressure gradients because the two tube openings may be in streams of different total pressure. This difficulty can be minimized, however, by locating the tube openings close together. Tests of several yaw-element tubes and yaw probes were included in the present investigation to define the parameters governing the flow-angle sensitivity of yaw probes.

The problem of designing a combination survey probe involves, therefore, the combination of these standardized methods of sensing flow angle and static and total pressure in such a manner that the mutual interference of the several individual sensing elements is negligible. The information obtained from the literature and from the present study was used in the design of the combination survey probes.

Reference 5 presents a combination probe similar to the final designs evolved from the present study, but no information other than flow-angle-indication sensitivity is provided. This particular probe would be generally unsatisfactory if constructed in very small sizes because the angle-sensing elements are difficult to locate accurately on its hemispherical nose.

The experimental work was performed primarily in a nonreturn instrument-calibration tunnel having an 8-inch-diameter test section. Twenty-nine different probes were used during the investigation. The characteristics of various types are presented and discussed. Two survey-probe types were tested in an actual testing installation.

SYMBOLS

p_s	static pressure
p	yaw- or pitch-tube pressure
H	total pressure
q	dynamic pressure, $H - p_s$
X	probe longitudinal axis
Y	probe stem axis
Z	axis normal to plane of X- and Y-axes
ψ	angle of yaw; rotation about Y-axis

θ angle of pitch; rotation about Z-axis

Subscripts:

o reference value

1,2 tube number

3 standard static probe

4 longitudinal static probe

APPARATUS AND TESTS

Testing Facility

The small wind tunnel designed and used for this probe calibration work is shown pictorially and schematically in figures 1 and 2, respectively. The air is induced from the atmosphere through a honeycomb straightener and two fine mesh screens and is then accelerated through a smoothly faired entrance cone into the test section. The test section is 32 inches long and $8\frac{1}{8}$ inches in diameter with machined and lacquer-coated internal surfaces. After the air passes through the test section, it is diffused and then passed through the rotor and exhausted to the atmosphere. The tunnel provides flow velocities up to 500 feet per second.

A longitudinal static-pressure probe extending a considerable distance upstream and downstream of the test section is suspended on piano wires 2 inches from the lower surface as shown in figure 2(b). This probe has four small static-pressure orifices 90° apart. The orifice position can be adjusted upstream or downstream of the instrument ports to indicate the true static pressure at any longitudinal position desired. The longitudinal static-pressure survey of the tunnel (fig. 3(a)) was made with this probe. The flow traverses of the tunnel, (figs. 3(b) and 3(c)) were made with calibrated pitot-static and claw-type yaw probes. The stems of the probes extended all the way across the test section so that the flow constriction would not vary as the probe traversed the tunnel. The results of these surveys for three flow speeds indicate that uniform flow existed in the tunnel except near the walls. The maximum variation of static or total pressure, in the middle 6 inches, is less than 1/2 percent of the dynamic pressure.

Instrument Mounting

Instruments can be mounted through three $1\frac{1}{2}$-inch-diameter split plugs, located 90° apart, 24 inches downstream of the test-section entrance (figs. 1 and 2(b)). All probes were mounted in the center of the test section if possible. Two instrument mounts of the type shown in figure 4(a) were made for use in these investigations. These bases permitted yaw-angle settings within 0.1° for 360° rotation and 10 inches of movement of the supported shaft to 0.01-inch accuracy. Each mount is equipped with a precision level to aid in alining the probe. Pitching and rolling mounts, as shown in figures 4(b) and 4(c), were used in conjunction with these bases for tests requiring pitching and rolling of the probe.

Probes Investigated

All instruments tested had either $\frac{1}{8}$- or $\frac{1}{4}$-inch-diameter stems. Figure 5 shows the four yaw-element probes and five claw-type yaw probes used in the yaw-sensitivity tests. The yaw-element probes were made from tubing of 0.050-inch outside diameter and 0.040-inch inside diameter and had slanted ends cut 90°, 60°, 45°, and 30° from the tube axis. Claw-type yaw probes having 180°, 150°, 120°, 90°, and 60° included angles between the forward arms were tested with included angles between the open faces cut successively to 0°, 15°, 30°, 45°, 60°, 90°, and 120°. For all the claw-type-probe tests the distance between the tube openings was approximately 1 tube diameter or 0.060 inch.

The six pitot-static probes tested are shown in figure 6 with the sliding sleeve and stem extensions used in conjunction with the probes for determining interference effects. These probes were made of tubing of 0.060-inch outside diameter with 0.020-inch internal pressure lines. The static-pressure orifices had a diameter of 0.006 inch and were located 10 tube diameters downstream of the tip. The stem center line was 0.5, 0.8, 1.2, 1.7, 2.3, and 3.0 inches downstream from the static-pressure orifices. The $\frac{1}{4}$-inch-outside-diameter sleeves were designed to fit over the probe stems of $\frac{1}{8}$-inch outside diameter to simulate a larger shaft and were slotted 4 inches to allow movement beyond the probes.

Eight types of combination probes (fig. 7) for sensing flow angle and total and static pressure were also tested. Although these probes were generally unsatisfactory, these test results provided information used in the design of the more accurate prism and pyramid types of com-

bination probes (fig. 8). The prism-type probe is designed to measure flow direction in one plane and total and static pressure. The pyramid probe is designed to measure flow direction in two planes and total and static pressure.

Tests and Presentation of Data

With the exception of tests of the pyramid-type probe at supersonic velocities and tests of the prism-type probes at high subsonic velocities, the tests were made in a speed range of 125 to 445 feet per second (a Mach number range based on standard stagnation temperature of approximately 0.1 to 0.4). The Reynolds number range based on standard stagnation density and viscosity and probe diameter was approximately 3,000 to 53,000.

Figure 9 shows the angle designations used in this paper. The pressure values used as references in this investigation were measured at a station midway between tunnel center line and wall. The reference static pressure was measured by either the longitudinal probe (fig. 2(b)) or the standard static probe (fig. 10), since the agreement between the probes was within 1/2 percent of dynamic pressure (fig. 11). The longitudinal probe was used predominantly, however. The reference total pressure was obtained with a yaw-element probe ($A = 90^\circ$, fig. 12).

Precision

Tests were made to determine the combined effect of blocking and proximity interference of a probe on the reference static pressure. For these tests, the dynamic pressure in the tunnel was adjusted by reference to a static-pressure orifice approximately $2\frac{1}{2}$ tunnel diameters upstream of the test section. The longitudinal-probe static-pressure reading was taken with a test probe inserted alternately from the top or from the side and without a test probe. The effect of the probe and stem caused the static-pressure reading of the longitudinal probe to change by less than 1 percent of the dynamic pressure for either probe position. The proximity interference of probes 5 or more probe diameters apart has been shown to exhibit no significant mutual interference effects (ref. 6). The probes studied in this investigation were located about 20 probe diameters from the reference. Therefore, the effect measured was due to blocking of the test section by the stem and probe, and since the effect of blocking was felt uniformly across the test section, no significant error in calibration of the test probes was anticipated.

All data, except those recorded in the supersonic tests, were read manually, the observer reading the vertical manometer to the nearest 0.01 inch of alcohol. For most tests where small differences of readings were needed, pressure lines were branched and an inclined U-tube was used to read these differences directly. All faired calibration curves are believed to be accurate within 1 percent of the dynamic pressure. Flow angles were read to the nearest 0.1°, but calibration curves may be in error as much as $1/4^\circ$ because of accumulative errors.

RESULTS AND DISCUSSION

Probe Sensitivity to Flow Angularity

In order to select suitable configurations for the yaw-sensing elements of combination survey probes, yaw elements and complete yaw probes were tested over a range of flow angles. The pressures at various yaw angles measured by the four yaw-element probes (fig. 12) are shown in figure 13. High-sensitivity yaw indication can be obtained by using tubes parallel to the flow and having ends slanted 30° to 60° relative to the tube axis. Each tube is seen to indicate total pressure when the face of the opening is normal to the flow. For other yaw angles, the inclination of the face of the opening relative to the probe axis influences the pressure reading. All four probes show high sensitivity to yaw when the face of the opening is between about 30° and 90° from normal to the flow direction. Consequently, this is the best range for use in designing sensitive flow-angle probes.

The results of tests to determine the sensitivity of various claw-type probes (fig. 14) are shown in figure 15. The claw-type probes are for measuring flow angle only. The sensitivity was obtained by recording the pressure readings of both yaw tubes at 5° above and below the null position. The sensitivity of all thirty-five configurations investigated was high enough for most uses. The yaw probe with tubes meeting at an angle of 120° and having open faces 15° (total angle $B = 30^\circ$) from the flow direction was the most sensitive. For this design, a change in yaw angle of 1° produced a difference in the two tube pressures of 9.5 percent of the dynamic pressure.

Effect of Stem on Static-Pressure Reading

The stem supporting a survey probe influences the flow field of the probe. The primary quantity affected by the stem is the static-pressure reading. In order to determine the allowable stem size, $\frac{1}{8}$- and $\frac{1}{4}$-inch stems were tested to measure the influence of the stem on probe readings. The details of the pitot-static probes tested are presented in figure 16.

The effects on pitot-static probe reading caused by $\frac{1}{8}$- and $\frac{1}{4}$-inch-diameter supporting stems were determined in the following manner: A $\frac{1}{4}$-inch sleeve placed around the $\frac{1}{8}$-inch stem (which extended completely across the tunnel) was moved toward and past the probe. The results of this test are shown in figure 17. The values at the end points are a measure of the effect of increased stem diameter on static-pressure reading. The left-hand side of the curves indicates the static-pressure error caused by the $\frac{1}{8}$-inch-diameter stem. For a $\frac{1}{2}$-percent error, the orifice location from the stem center line should be about 14 stem diameters. The effect of the $\frac{1}{4}$-inch-diameter sleeve is seen to begin when the sleeve is within $1\frac{1}{2}$ inches of the probe. This effect increases until the sleeve is advanced approximately $1\frac{1}{2}$ inches beyond the probe, after which little change is noted. The magnitude of the errors is largest for the shortest probes, but even the longest is slightly affected by the $\frac{1}{4}$-inch-diameter stem. When the end of the $\frac{1}{4}$-inch sleeve is even with the probe, the influence of the sleeve on the probe static-pressure reading is seen to be approximately one-half of the total effect. The $\frac{1}{4}$-inch-diameter stem produced approximately three times as much static-pressure error as the $\frac{1}{8}$-inch stem; thus the importance of using small stems is emphasized. The effect of flow velocity on these results was measured for a typical configuration and found to be small within the range tested (fig. 18).

For combination probes of approximately the same size as these pitot-static probes, the results of these tests indicate that $\frac{1}{4}$-inch-diameter stems can be tolerated at distances greater than $1\frac{1}{2}$ inches from the probe, provided that the stem near the probe is slender.

Combination Probes

Preliminary designs.- In the process of obtaining the final designs, several probes were investigated. Probe A (figs. 7 and 19) can be used successfully in uniform flow fields if a static-pressure correction is made (fig. 20). However, the correction usually varies with flow velocity more than is indicated for this particular probe, the tubes

are easily bent so that the static-pressure calibration or yaw null point or both is changed, and because of the spread of the elements the probe should not be used in nonuniform flow fields. Probes B to H (figs. 7 and 21 to 27) were considered inadequate and rejected because of static-pressure error, flow-angle-indication error, or low flow-angle-indication sensitivity. The results obtained in tests of these probes are presented in table I and are of interest because some of these probes are in common use. These results also point out that clean aerodynamic design is necessary to eliminate mutual interference effects between the various elements and to produce a satisfactory probe.

Prism-type probe.- Reference 1 indicates that the nose shape of a pitot-static tube has little influence on the indicated total pressure. Reference 4 shows for several nose shapes that a static-pressure error of less than 1 percent of the dynamic pressure may be expected at small tube attitudes if the static orifices are 3 or more probe diameters downstream of the base of the nose. If the yaw-tube openings are installed in the nose of the pitot-static tube, the accuracy of the total- and static-pressure indication would be maintained and the angle of yaw could be sensed in an undisturbed stream. This reasoning led to the design of the prism-type probe (figs. 8 and 28) which contains most of the desired features of survey probes. The total-pressure tube is centrally located and in the region of undisturbed flow. The yaw tubes are placed so that they also sample undisturbed and undivided flow. The tubes are only 0.040 inch apart; therefore they are little affected by nonuniform flow fields unless the gradient is large. The yaw-tube surfaces in the nose of the probe are inclined 30° from normal to the flow to provide high sensitivity; these surfaces are flat so that small errors in locating the tube openings will not involve large changes in calibration. The static-pressure orifices are located over 3 probe diameters downstream of the base of the nose in a region where the static-pressure error was found to be very small. The supporting stem is narrow for a distance of $1\frac{1}{2}$ inches from the probe to minimize stem interference effects. The probe is small (fig. 28) and permits the simultaneous measurement of flow pressures and angularity within axial and radial distances of 0.5 and 0.09 inch, respectively.

The static-pressure error of the prism-type probe was measured by using both the standard and the longitudinal probes for reference. Figure 29 shows that the maximum error indicated by both curves for flow velocities up to 445 feet per second is less than 1/2 percent of dynamic pressure. Zero variation of yaw null point up to 445 feet per second was observed. The sensitivity of the probe to yaw was obtained at two flow velocities, 197 and 390 feet per second (fig. 30). Only small changes in results were noted as velocity was varied; both tests show high flow-angle-indication sensitivity and both static- and total-pressure errors below 1/2 percent of the dynamic pressure until the

probe was yawed ±5°. Probe sensitivity to pitching was also measured at two speeds, 196 and 308 feet per second (fig. 31), and a maximum static-pressure variation of $1\frac{1}{2}$ percent of the dynamic pressure was observed up to pitch angles of ±5°.

In order to determine the trend of the static-pressure error of the prism-type probe in the Mach number range from 0.3 to 0.8, a probe was tested in an annular passage of 12-inch inner diameter and 16-inch outer diameter upstream of a high-speed rotor. The static-pressure error measured relative to that at a wall tap in the passage was found to be reasonably constant up to a Mach number of about 0.5 and comparatively equal to values presented in figure 29. Beyond a Mach number of 0.5, the error gradually increased and was enlarged by approximately 1 percent of the dynamic pressure at a Mach number of about 0.8.

Prism-type probe designed to be mounted on a rotor.- Figure 32 shows a variation of the prism-type probe that was designed to be mounted directly on a rotor to measure exit angles behind a blade row. Because of the heavier supporting stem, a static-pressure correction of about 2 percent was found, but other characteristics remained essentially the same (fig. 33). As evidence of the consistent accuracy of both prism probes, turning angles were measured at three diameters on a rotor in the velocity range from 154 to 194 feet per second by using both probes (figs. 34 and 35). Nearly identical turning angles were obtained using the stationary and rotor-mounted probes. These two probes and two other prism probes have been used for many tests and have provided consistent and accurate results. The conclusion is reached that this design is favorable for general use.

Short prism-type probe.- A short prism-type probe (fig. 36) was designed for surveying the flow in a multistage compressor where the space between blade rows is less than 1.46 inches, the length of the standard prism probe. The static-pressure calibration against flow velocity (fig. 37) indicates that locating the stem about 5 probe diameters closer to the static orifices and the static orifices $1\frac{1}{2}$ probe diameters closer to the nose requires an approximately constant static-pressure correction of about 1.8 percent of the dynamic pressure in the velocity range tested. This probe was also checked in an annulus upstream of a high-speed rotor to determine the static-pressure-calibration trend in the Mach number range from 0.3 to 0.8. The static-pressure correction was found to be very nearly constant and consistent with values presented in figure 37 up to a Mach number of about 0.5. Beyond a Mach number of 0.5, the error starts to change and is altered in the positive direction by about 3 percent of the dynamic pressure at a Mach number of about 0.8.

Pyramid-type probe.- A special variation of the prism-type probe was constructed which contained two additional null tubes to obtain pitch angles. This pyramid probe, shown in figures 8 and 38, has the same general design features as the prism probe but can also indicate pitch angles by null positioning or by calibration. Although the heavier stem resulted in a more sturdy probe, it had practically no effect upon the performance characteristics. Figure 39 shows that the yaw and pitch null points and the very small static-pressure error vary only slightly with flow velocities up to 445 feet per second. The yaw and pitch sensitivities (figs. 40 and 41) indicate that the pyramid probe has the same favorable qualities as the prism probe and is, therefore, also recommended for general use. In order to obtain an indication of the static-pressure error at high speeds, the pyramid probe was tested downstream of the high-speed rotor in a Freon-12 atmosphere at Mach numbers up to 2.0. The static-pressure calibration for these tests was obtained by yawing, pitching, and rolling the pyramid probe to the null position at a given flow speed and then setting the standard static probe (fig. 10), which was placed at a different circumferential position in the same radial plane, at the same attitude and comparing the pressures indicated. The difference in static pressure indicated by the two probes is shown against approximate Mach number in figure 42. The accuracy of the standard probe is not known in the transonic and supersonic range. Although large errors were indicated near sonic velocity, the average difference is considered reasonably small. The figure also shows the results of a similar test on probe type G. The differences in static pressure between the standard probe and the probe type G are over twice as large, near sonic velocity, as the differences between the standard and pyramid probe. The pyramid probe can probably be used successfully at Mach numbers as high as 2 if careful calibration is made.

Instrument Response

Probes even smaller than the prism and pyramid probes tested are often needed. In order to determine the effect of scaling down these designs on reaction time, the average reaction time of the probes was compared with the reaction time for straight tubes of 12-, 6-, and 3-inch lengths and 0.040-, 0.020-, and 0.010-inch inside diameter. Reaction times were obtained in the following manner: One of the probes, which contained approximately 14 inches of tubing (3 inches of tubing of 0.020-inch inside diameter joined to 11 inches of tubing of 0.040-inch inside diameter), was connected through a 72-inch length of tubing of 0.22-inch inside diameter to a 0.156-inch-inside-diameter manometer tube 84 inches long. The pressure in this system was increased so that a deflection of 50 inches of alcohol was observed on the manometer tube. The pressure in the system was then allowed to return to its original level by a natural flow of air through the probe orifices. Manometer level readings were taken at even time intervals during this return. The reaction times of the straight tubes were obtained in the same manner.

The results shown in figure 43 indicate that any appreciable decrease in instrument size would considerably increase reaction time, and unless unusual pressure indicating devices were used, this increase would render significantly smaller designs unfit for normal testing.

CONCLUSIONS

Systematic investigations were made to obtain information for the design of reliable combination flow-surveying probes which indicate total pressure, flow angle, and static pressure at a single point, have negligible correction factors, and are suitable for subsonic turbomachine testing. As a result of these tests, the following conclusions were made:

1. High-sensitivity yaw indication can be obtained by using tubes parallel to the flow and having ends slanted 30° to 60° relative to the tube axis.

2. The maximum-flow-angle sensitivity for a claw-type yaw probe is obtained when the included angle between the two yaw-element tubes is 120° and the open faces of the yaw-element tubes are 15° (total angle, 30°) from the flow direction.

3. Combination flow-surveying probes were designed which can be used to measure flow angles in one or two planes as well as static and total pressure. The probes are small and permit simultaneous measurement of flow pressures and angularity within axial and radial distances of 0.5 and 0.09 inch, respectively.

Langley Aeronautical Laboratory,
National Advisory Committee for Aeronautics,
Langley Field, Va., August 13, 1952.

REFERENCES

1. Gracey, William, Letko, William, and Russell, Walter R.: Wind-Tunnel Investigation of a Number of Total-Pressure Tubes at High Angles of Attack. Subsonic Speeds. NACA TN 2331, 1951. (Supersedes NACA RM L50G19.)

2. Gracey, William, Coletti, Donald E., and Russell, Walter R.: Wind-Tunnel Investigation of a Number of Total-Pressure Tubes at High Angles of Attack. Supersonic Speeds. NACA TN 2261, 1951.

3. Merriam, Kenneth G., and Spaulding, Ellis R.: Comparative Tests of Pitot-Static Tubes. NACA TN 546, 1935.

4. Ower, E., and Johansen, F. C.: The Design of Pitot-Static Tubes. R. & M. No. 981, British A.R.C., 1925.

5. Bäuerle, H.: Measuring Instruments for Pressure, Velocity, and Direction Measurements. Reps. and Translations No. 951, British M.A.P. Völkenrode, Mar. 15, 1947.

6. Krause, Lloyd N.: Effects of Pressure-Rake Design Parameters on Static-Pressure Measurement for Rakes Used in Subsonic Free Jets. NACA TN 2520, 1951.

TABLE I.- INDICATING CHARACTERISTICS OF SEVEN COMBINATION PROBES TESTED

Combination-probe type			Static-pressure error, percent q (Probe nulled; Flow velocity, 295 fps)	Static-pressure error, percent q (Probe nulled; Flow velocity, 200 fps)	Incremental static-pressure error, percent q ($\psi = \pm 5^\circ$)	Average yaw sensitivity, $\frac{P_1 - P_2}{q}$, percent/deg	Reason design not satisfactory
	A, in.	B, in.					
B	0.060	0.056	-7.4	-7.0			Static-pressure error varies with flow velocity and dimensions A and B
	.060	.019	-1.15	-.75			
	.050	.016	0	.65			
C	Orifice location from nose, in.						Yaw sensitivity is too low and static-pressure error is erratic and unsymmetrical with yaw
	0.72		6.9		Large	0.3	
	.48		2.8		±1.5	.6	
	.24		1.5		±1.5	.2	
D	Orifice location from nose, in.						Yaw sensitivity is too low and static-pressure error is erratic and unsymmetrical with yaw
	0.50		1		$\left\{\begin{matrix} .8 \\ -3.0 \end{matrix}\right\}$	.5	
	.20		-2.2		$\left\{\begin{matrix} 1.7 \\ -9.0 \end{matrix}\right\}$	.9	
E			.6	.6	-.3	2.5	Yaw null angle varies ±6° with ±10° pitch
F			-2.0	-.6			Static-pressure error and yaw null angle vary with flow velocity
G			2.1	1.5			Static-pressure error varies with flow velocity and probe divides flow before flow angle is sensed
H			8.3	7.7			Static-pressure error is excessively high and varies with flow velocity

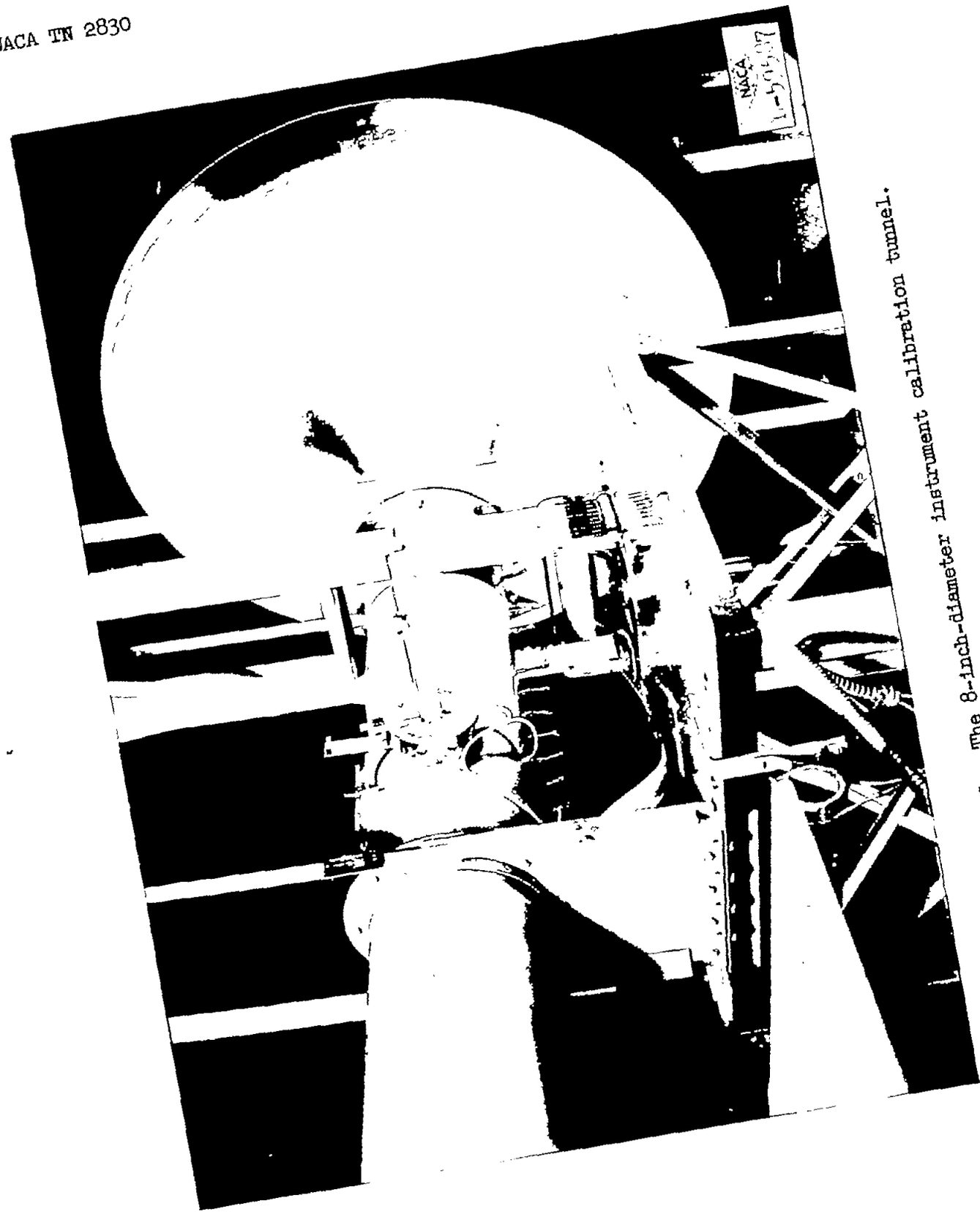

Figure 1.- The 8-inch-diameter instrument calibration tunnel.

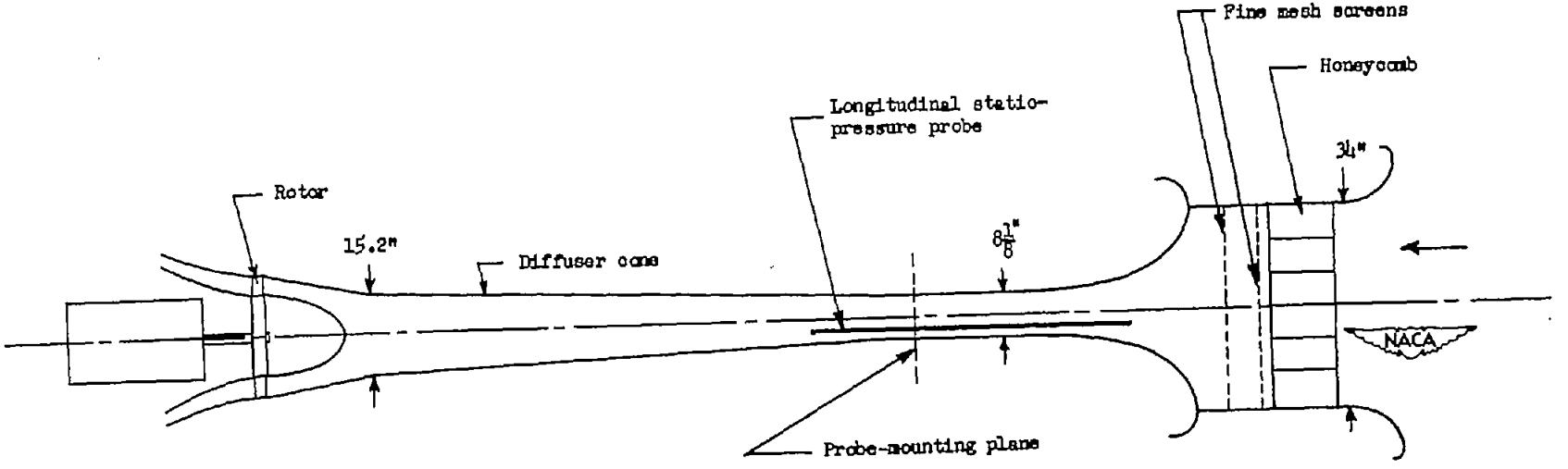

(a) General view.

Figure 2.- Eight-inch-diameter instrument calibration tunnel.

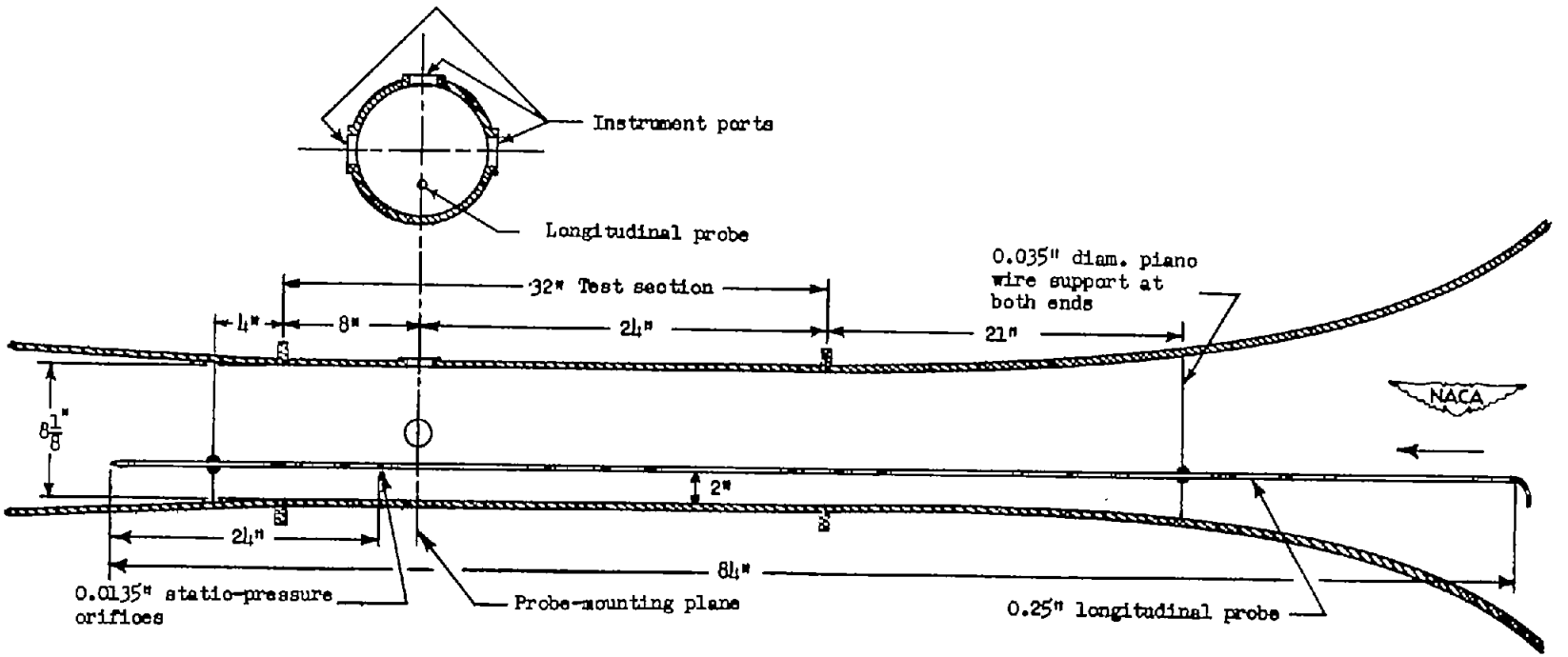

(b) Test section.

Figure 2.- Concluded.

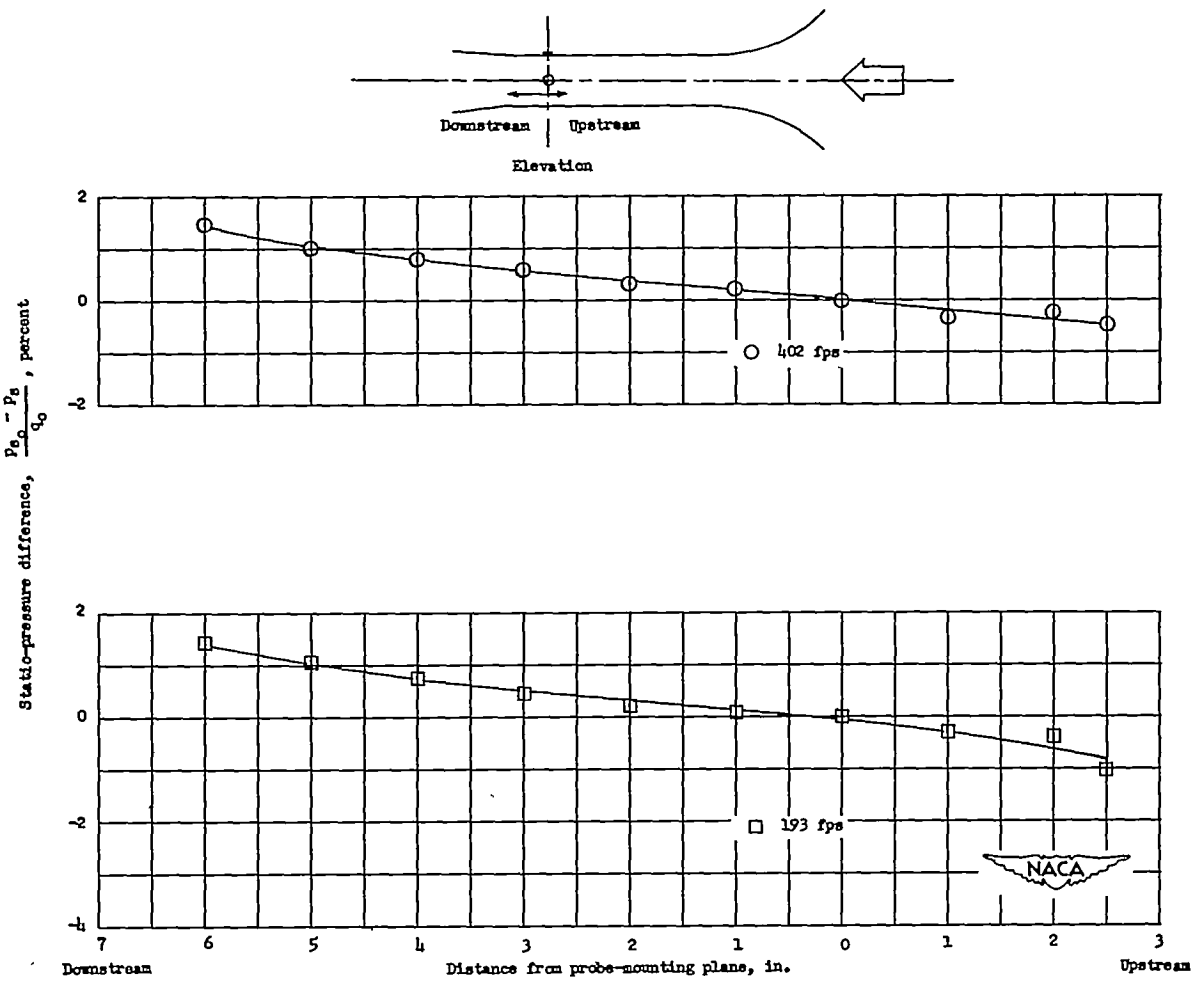

(a) Static-pressure variation along tunnel axis referred to value measured at probe-mounting plane.

Figure 3.- Flow condition in the instrument calibration tunnel.

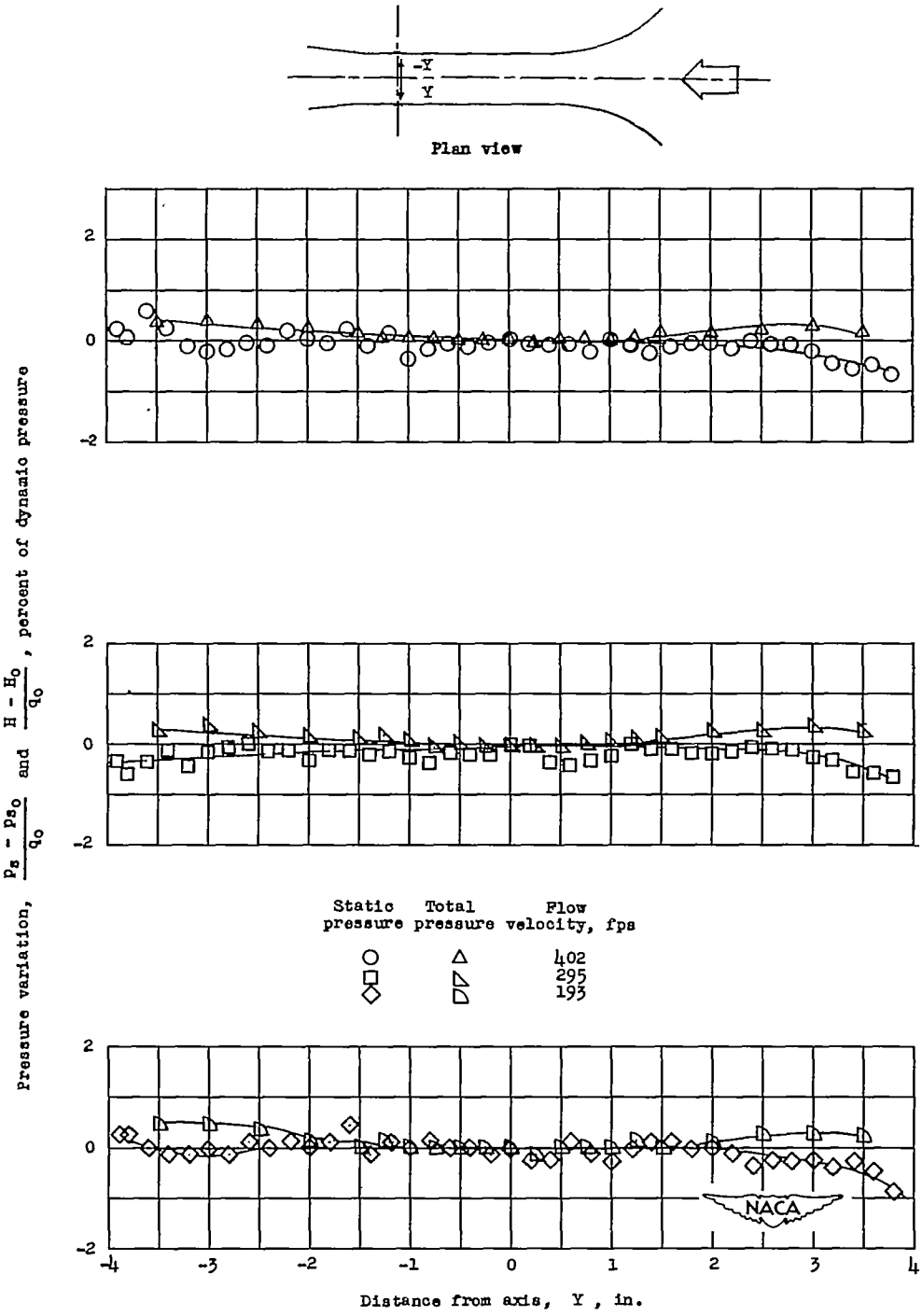

(b) Variation of static and total pressure across the tunnel at the probe-mounting plane referred to values measured at the axis.

Figure 3.- Continued.

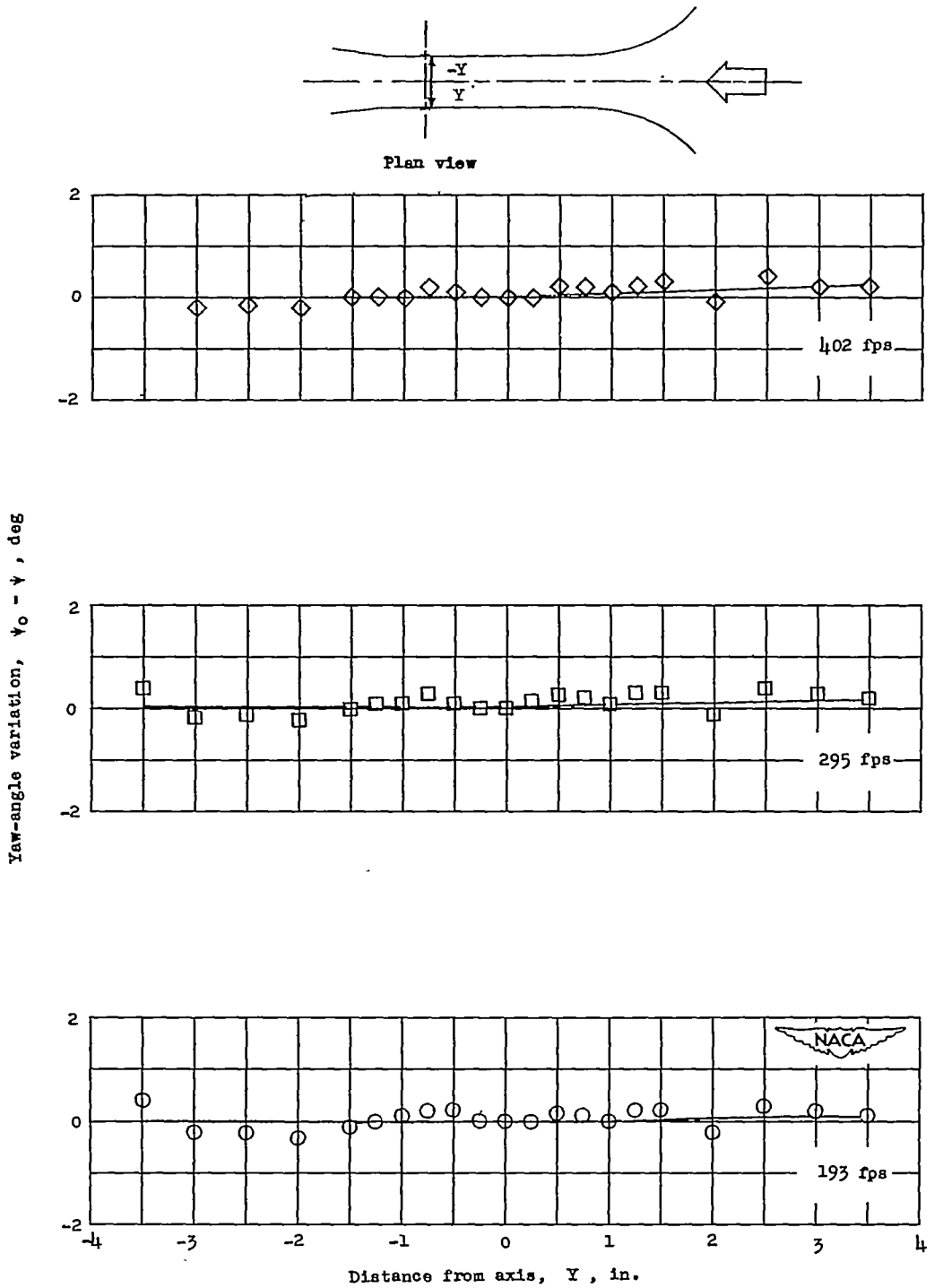

(c) Variation of yaw angle across the tunnel at the probe-mounting plane referred to values measured at the axis.

Figure 3.- Concluded.

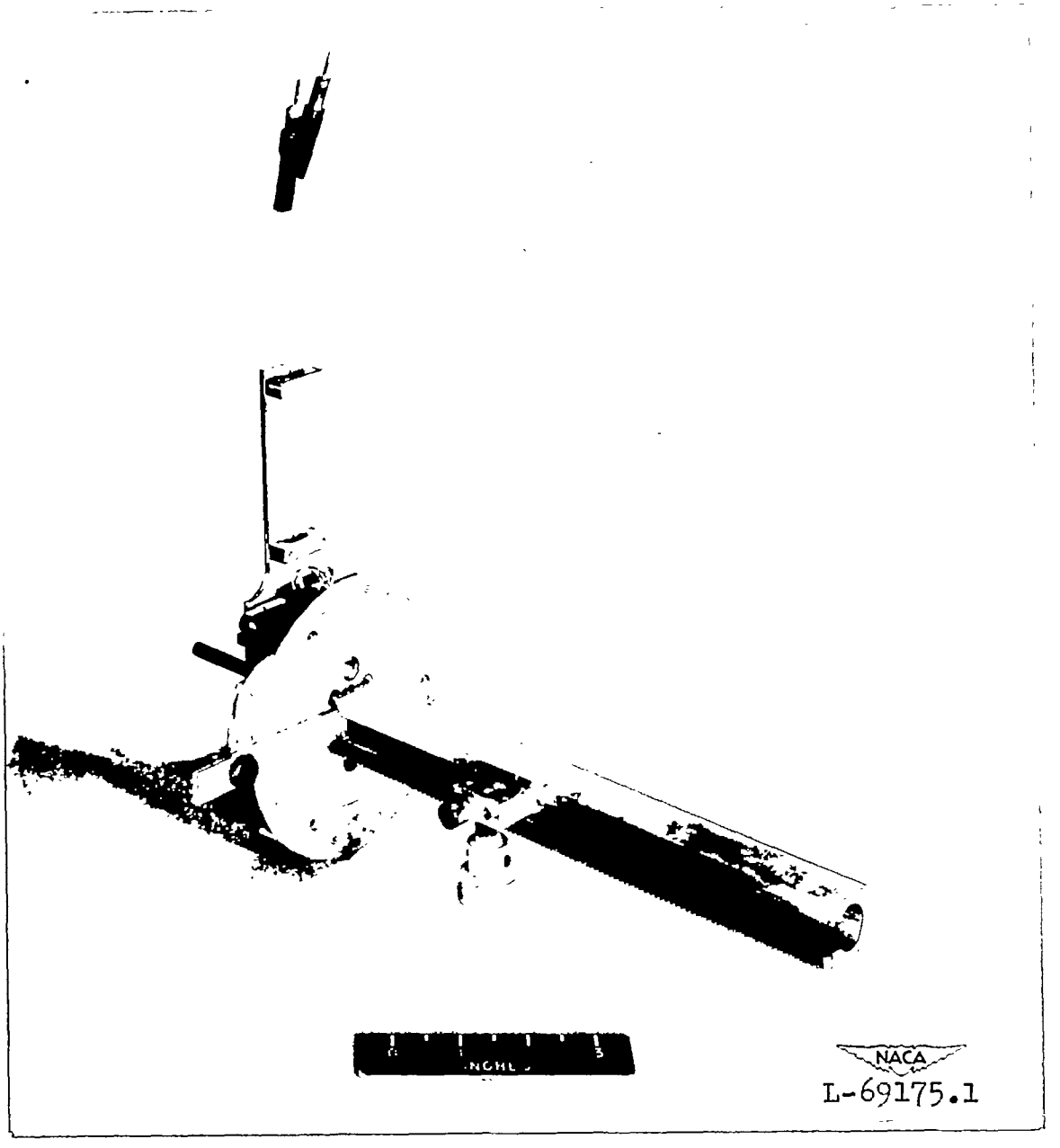

(a) Mount used to yaw test probes and traverse test section.

Figure 4.- Probe mounts.

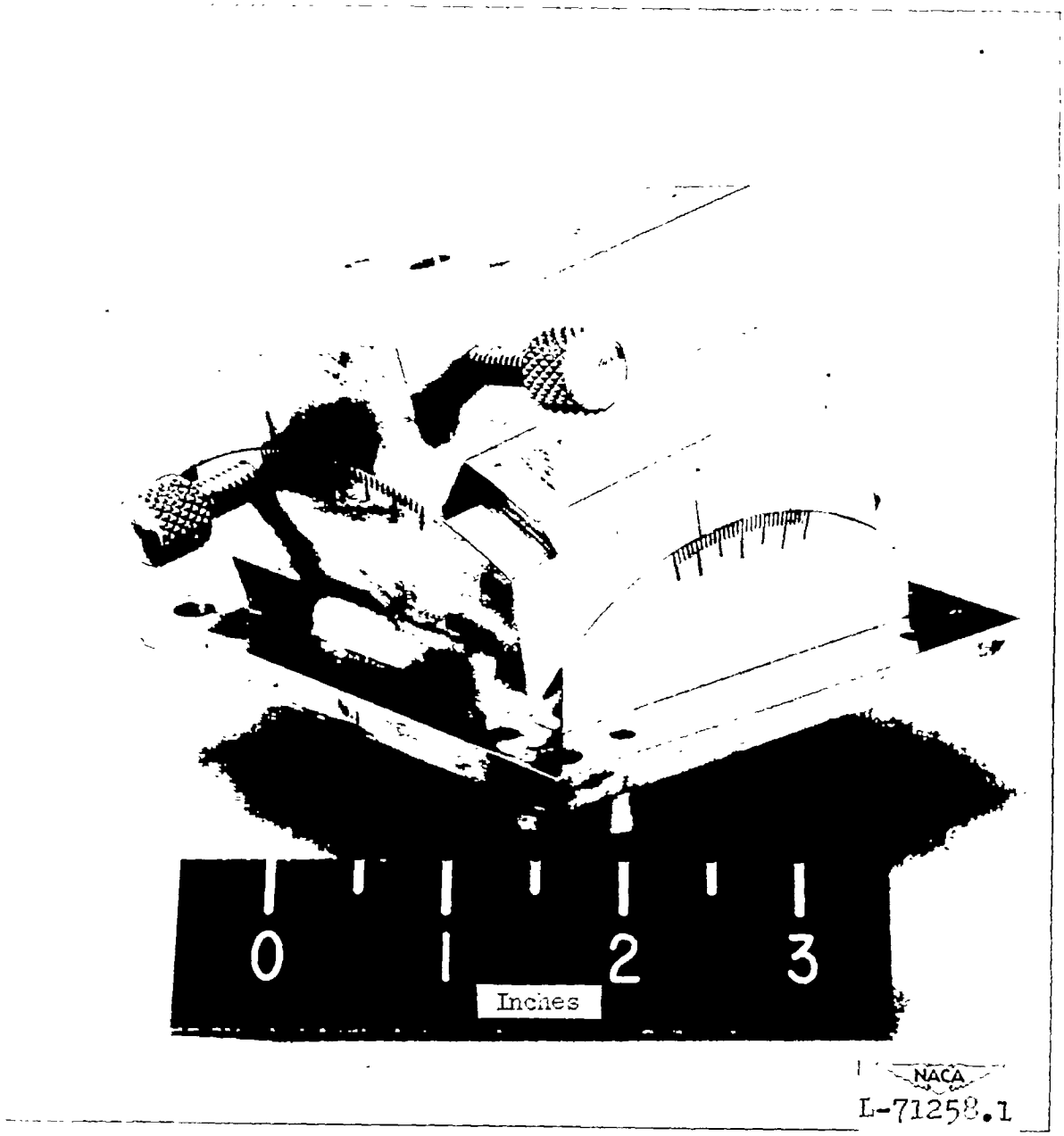

(b) Mount used to pitch and roll test probes.

Figure 4.- Continued.

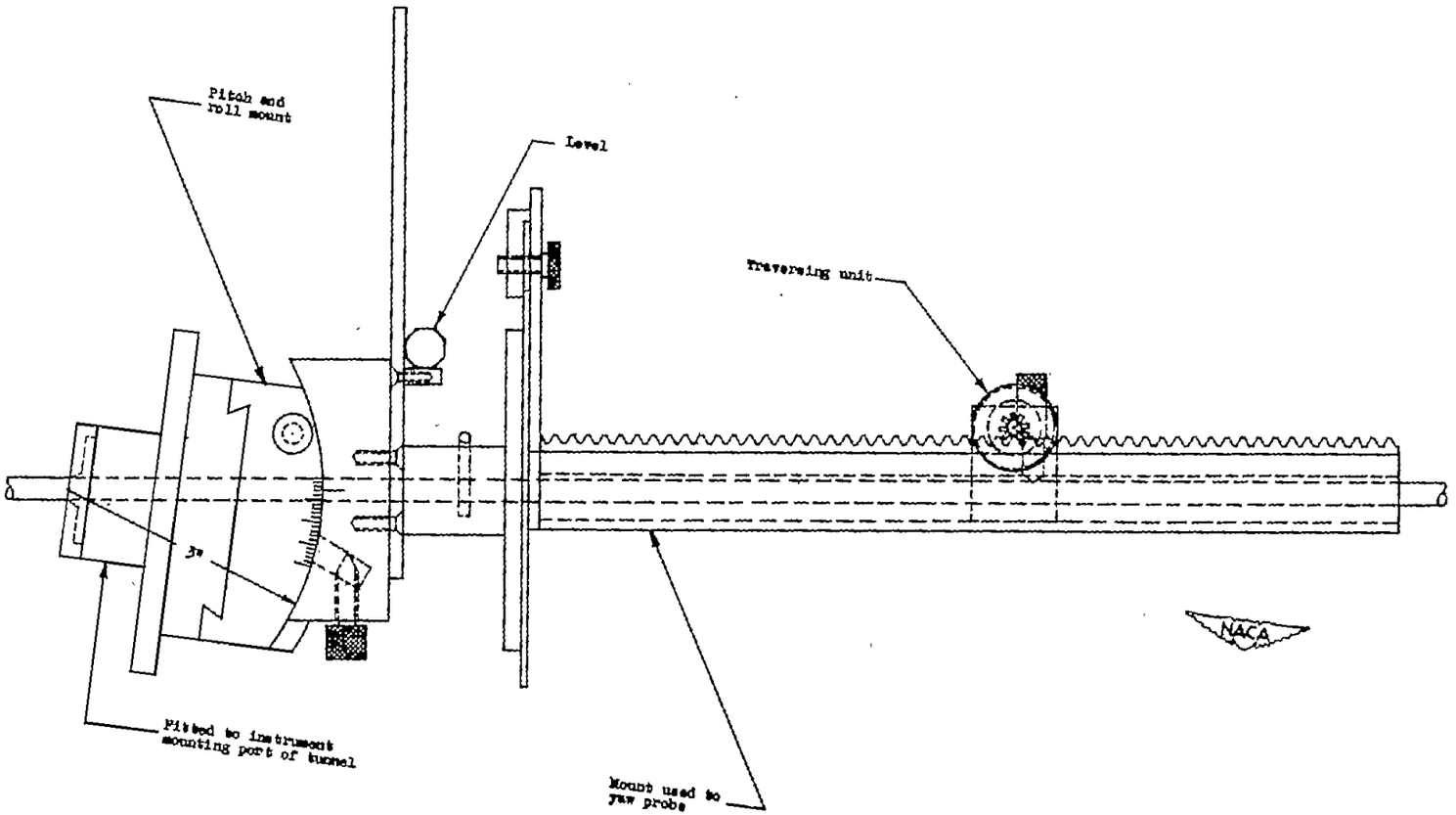

(c) Assembly.

Figure 4.- Concluded.

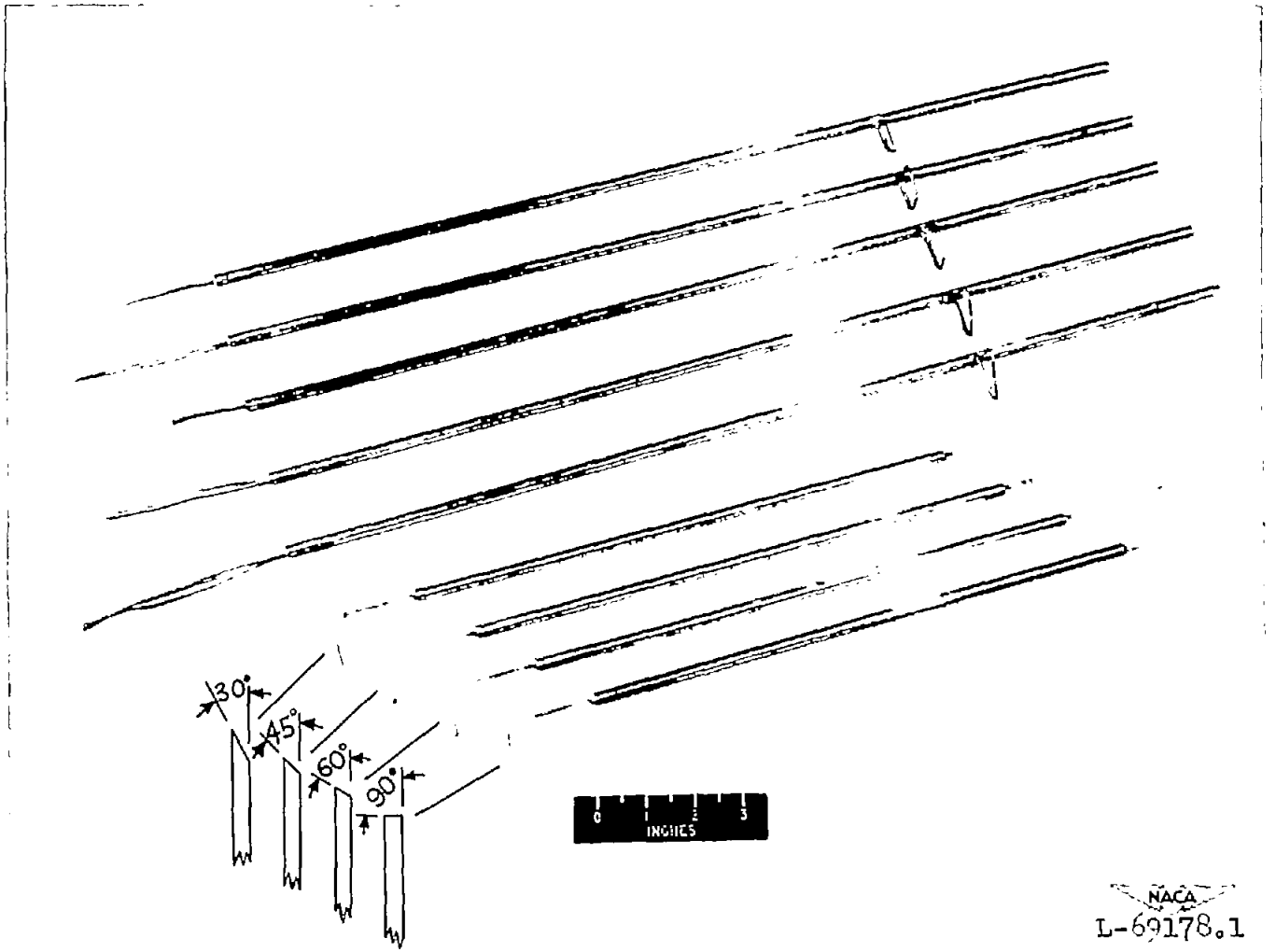

Figure 5.- Four yaw-element probes and five claw-type yaw probes used in this investigation.

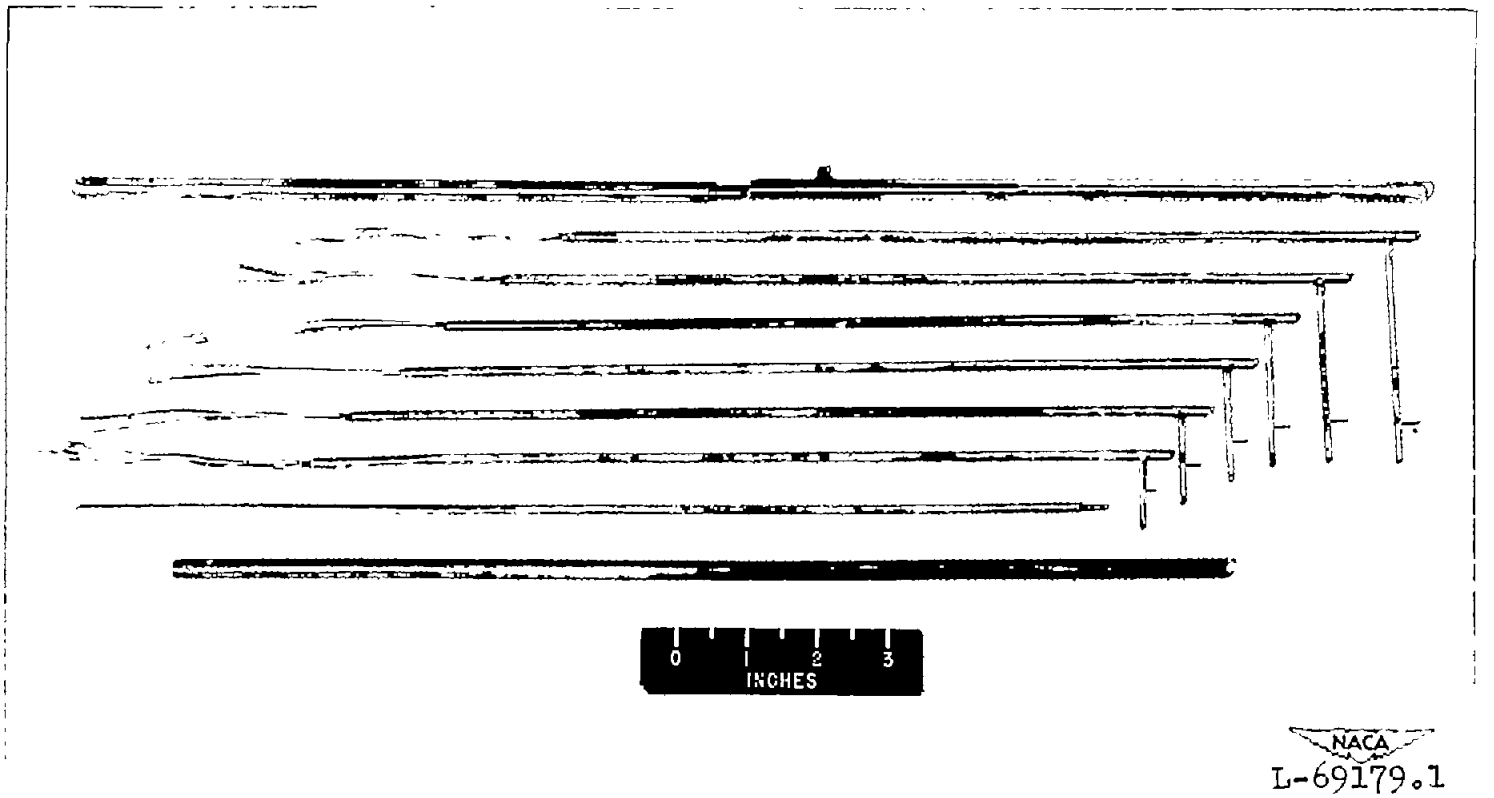

Figure 6.- Six pitot-static-pressure probes and the slotted sleeves and stem extensions used in the interference tests. Bars indicate location of static-pressure orifices.

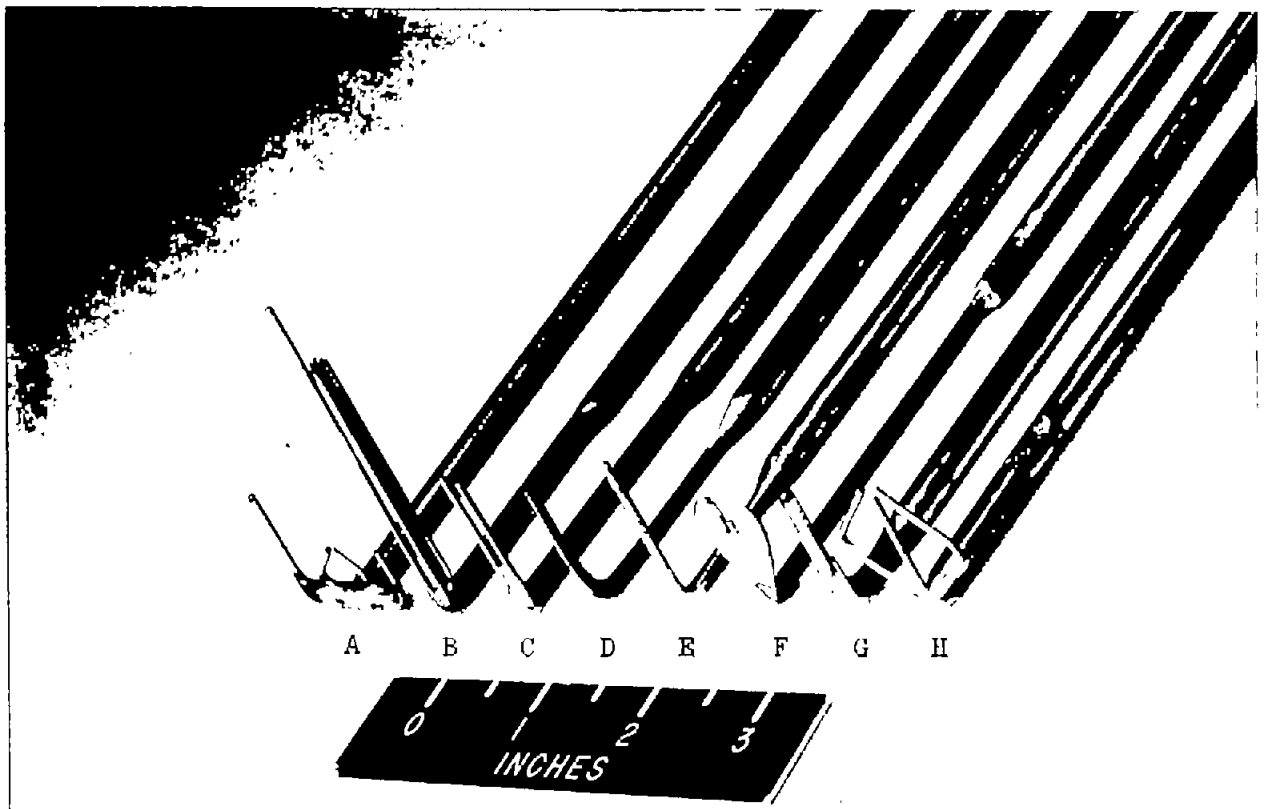

Figure 7.- Eight combination probes designed to measure flow direction and total and static pressure.

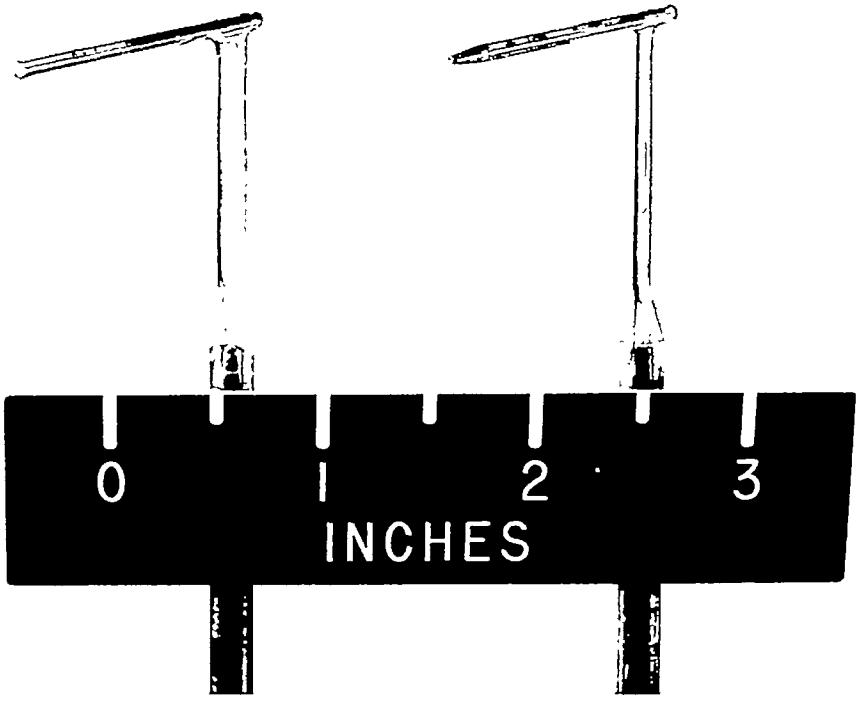

Pyramid Prism

Enlarged views of probe ends

NACA
L-71927.2

Figure 8.- Composite photograph of the pyramid and prism combination probes.

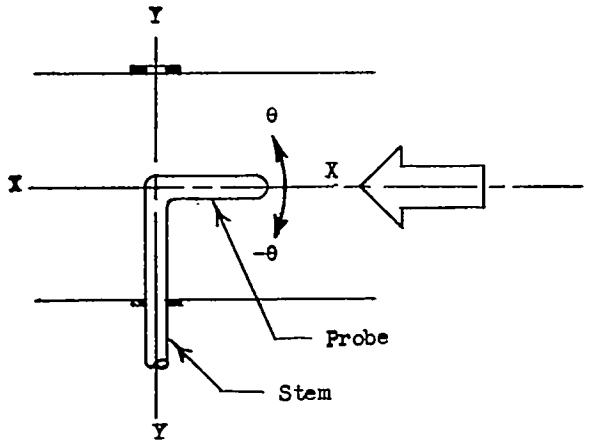

Plan view

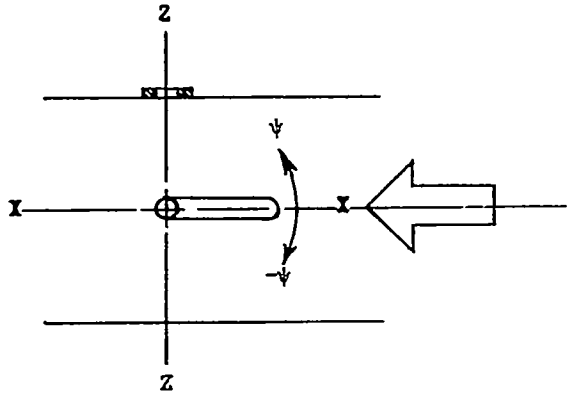

Elevation view

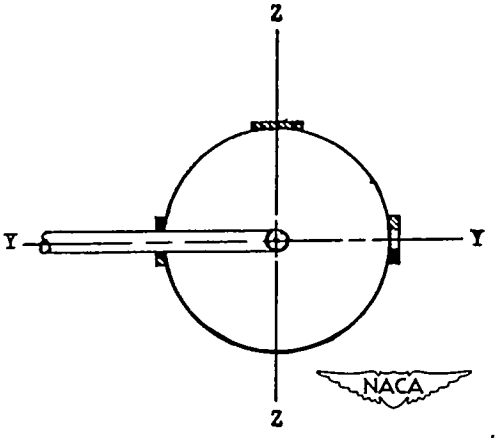

Profile view

Figure 9.- Sketch showing angle designation.

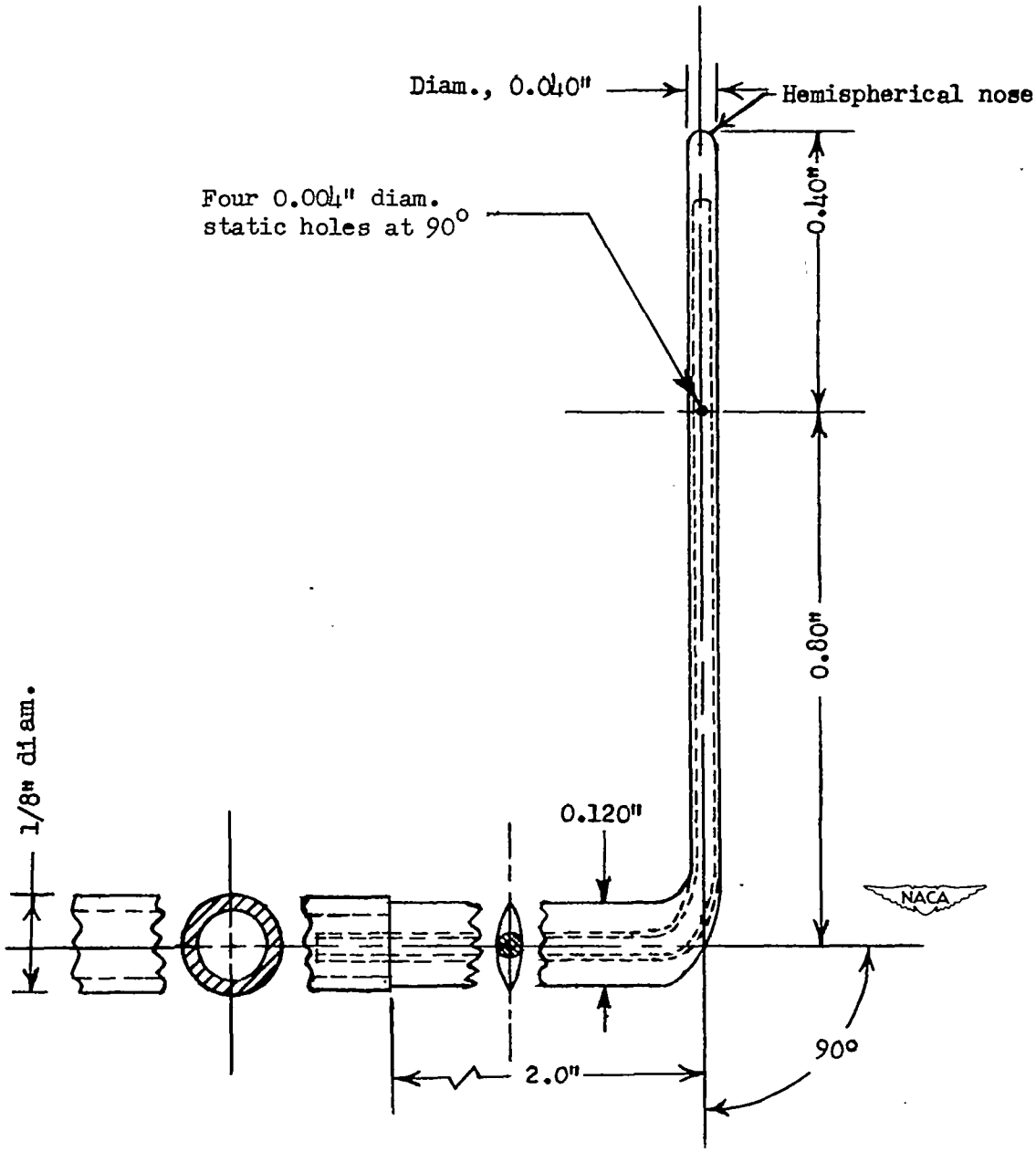

Figure 10.- Details of standard static probe.

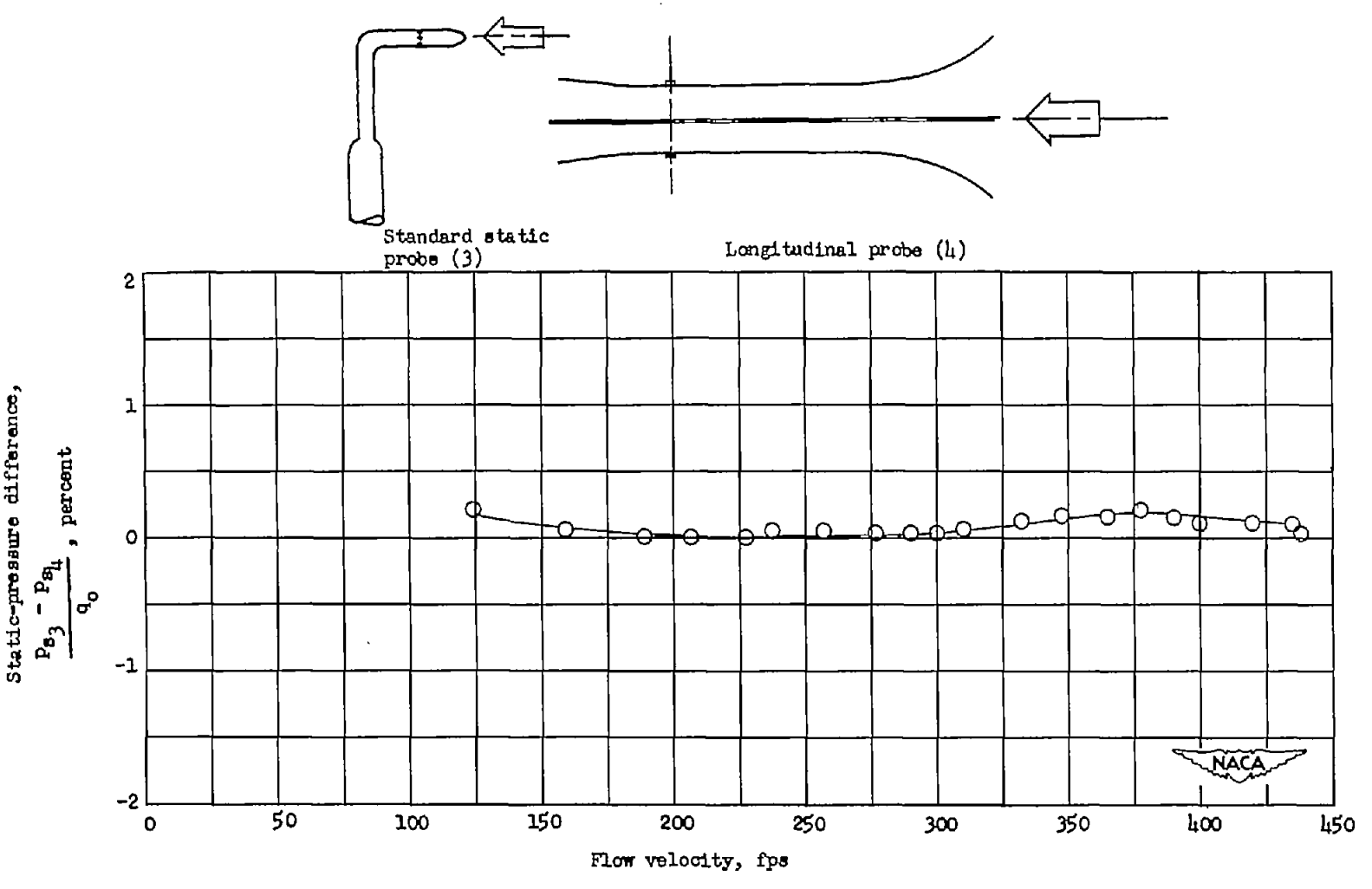

Figure 11.- Variation of difference in the static-pressure readings between the standard static probe and longitudinal probe with flow velocity.

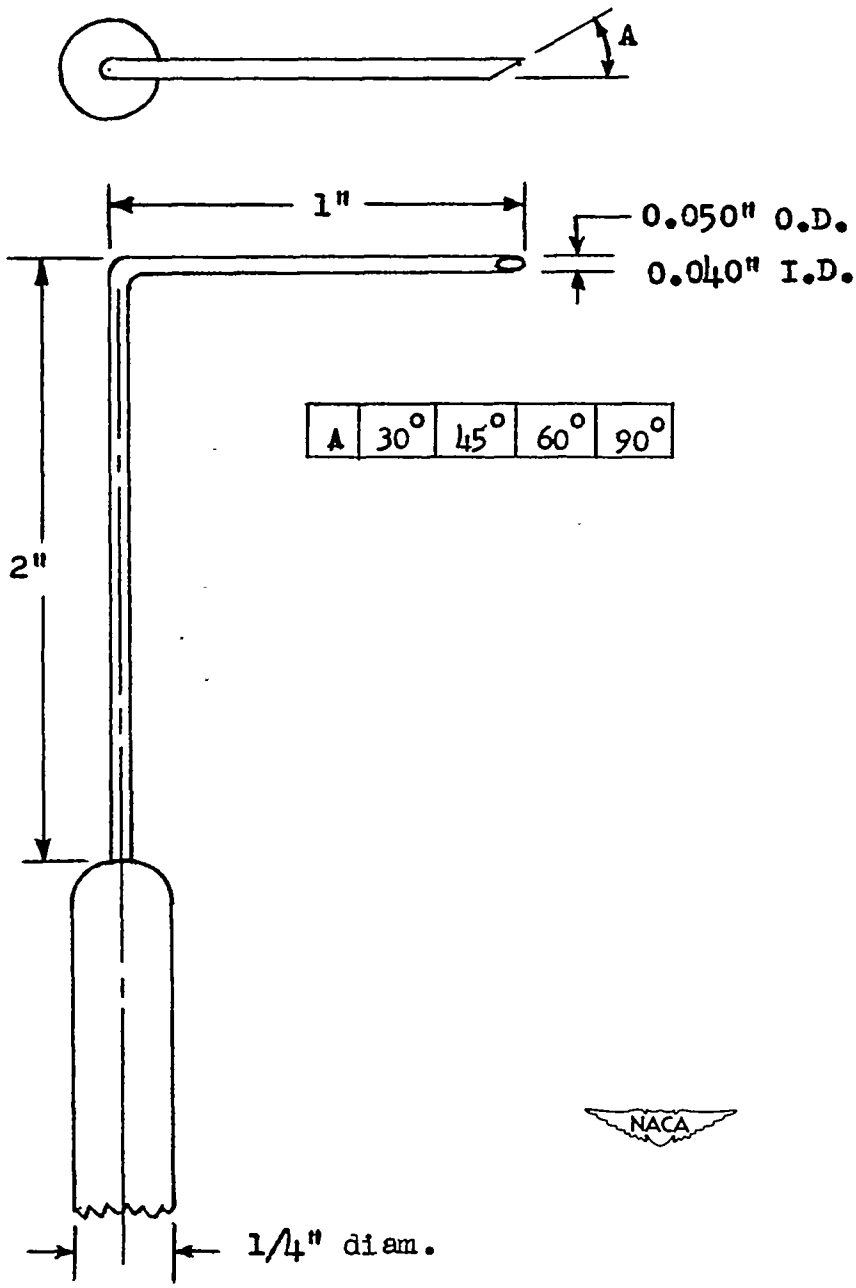

Figure 12.- Details of yaw-element probes.

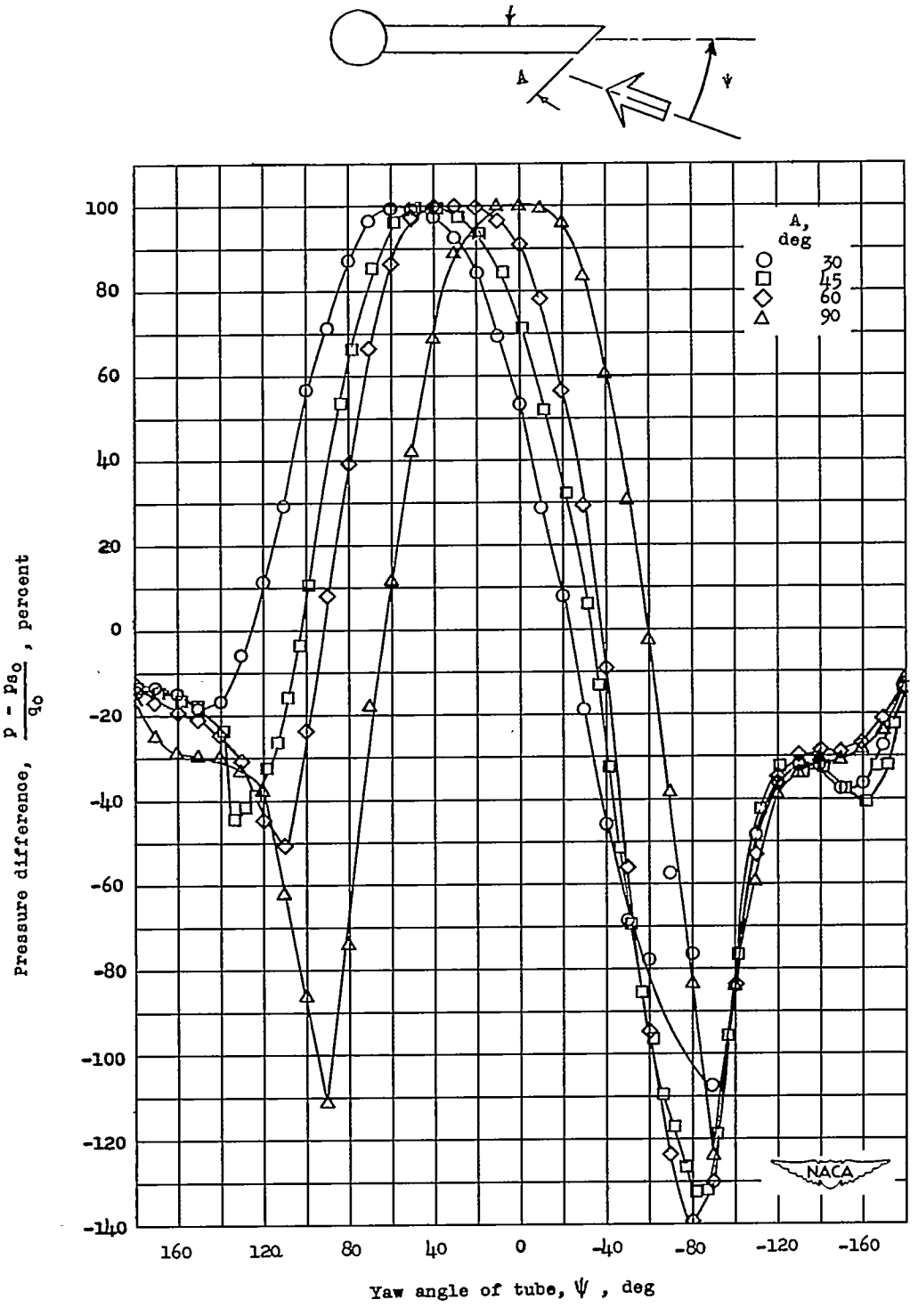

Figure 13.- Variation of difference in the tube pressure and static pressure between four yaw-element probes and longitudinal probe with yaw angle. Flow velocity, 295 feet per second.

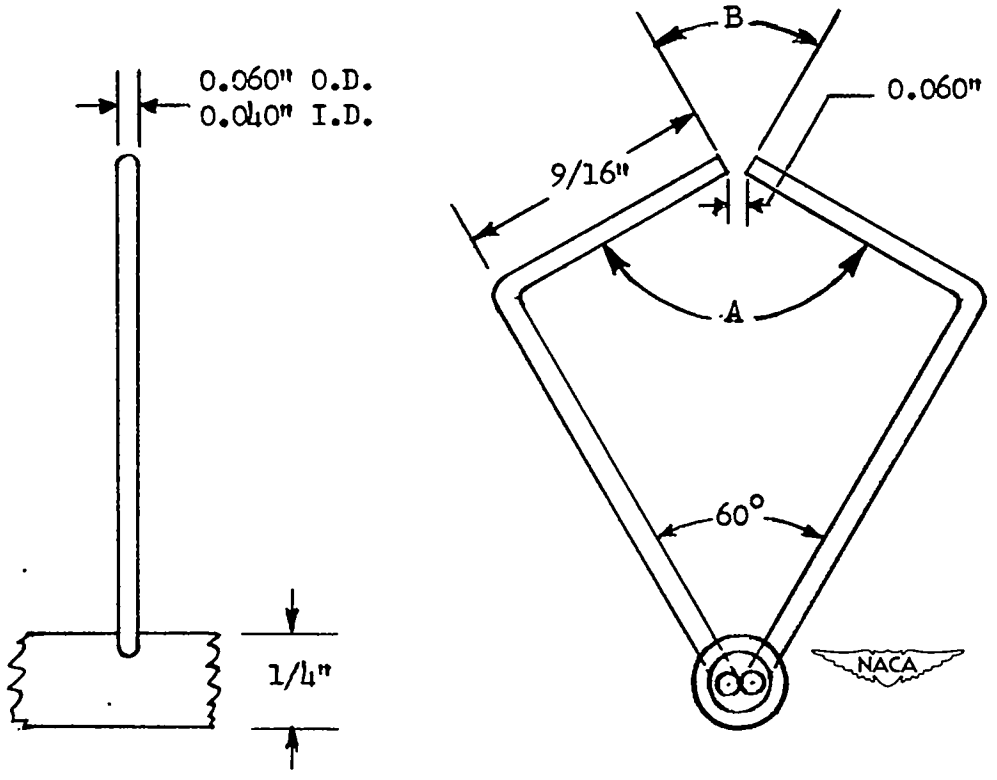

Figure 14.- Details of claw-type yaw probes.

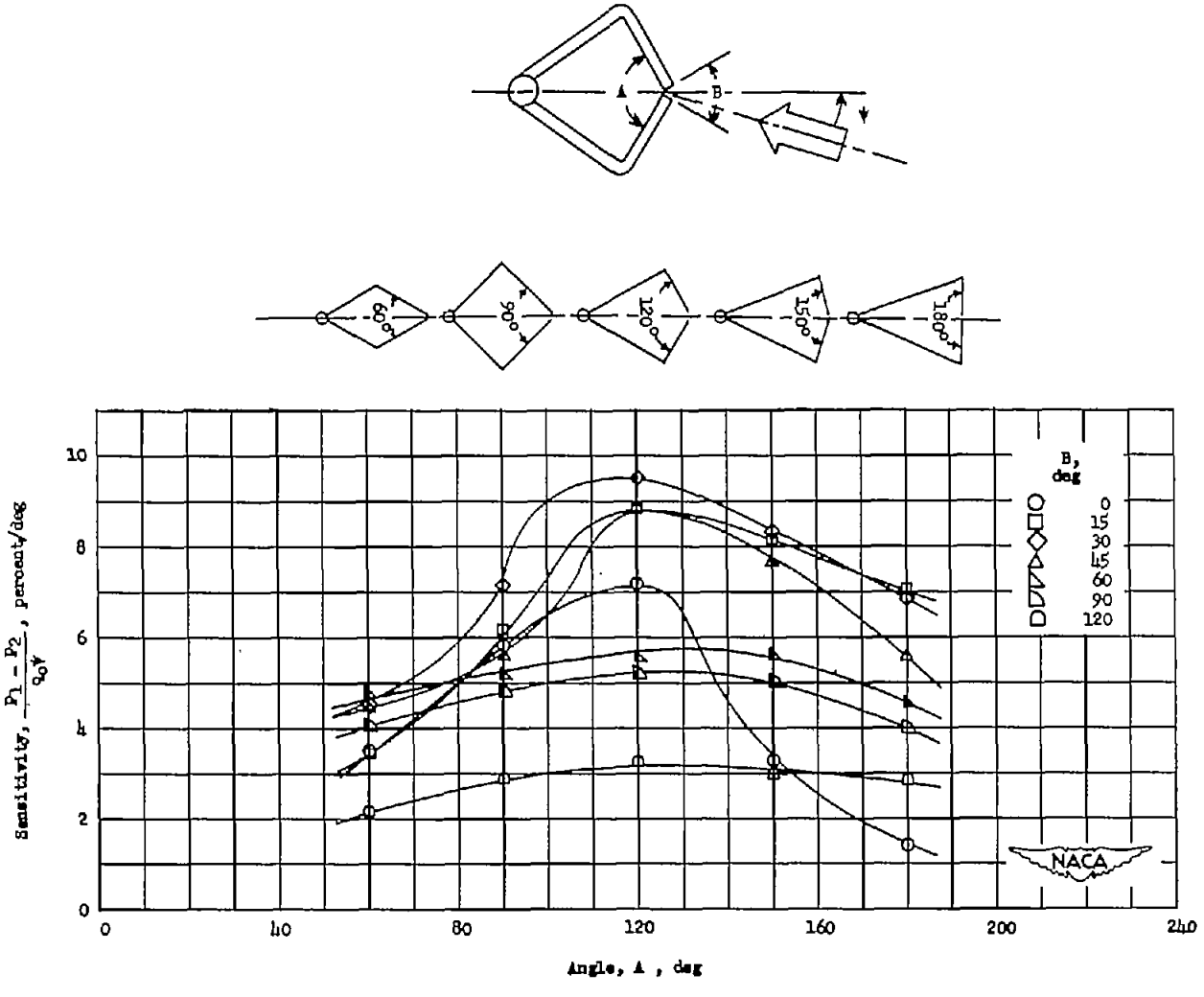

Figure 15.- Yaw sensitivity of claw-type probes. Flow velocity, 295 feet per second; $\psi \approx 0^{\circ}$.

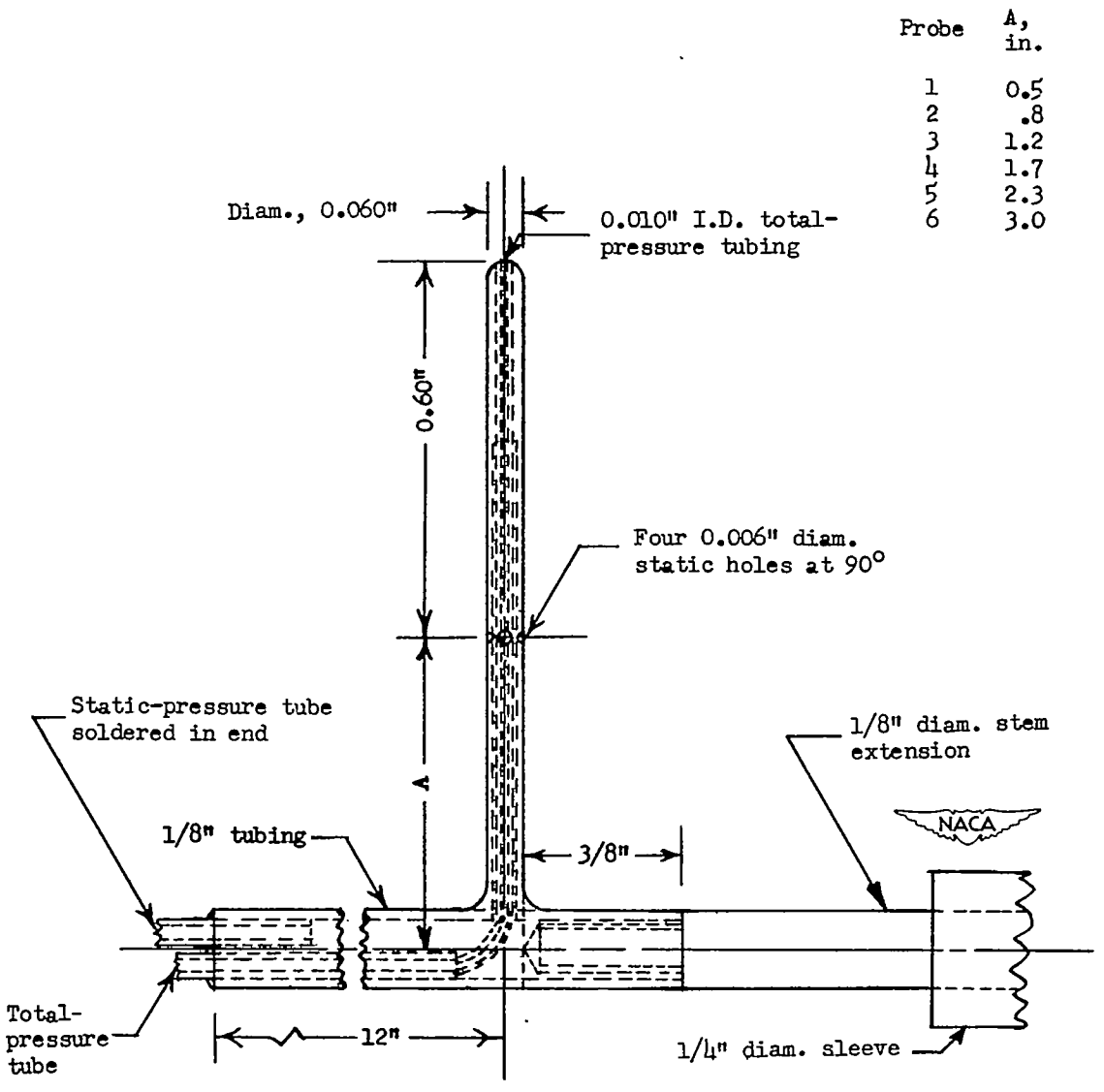

Figure 16.- Details of pitot-static probes.

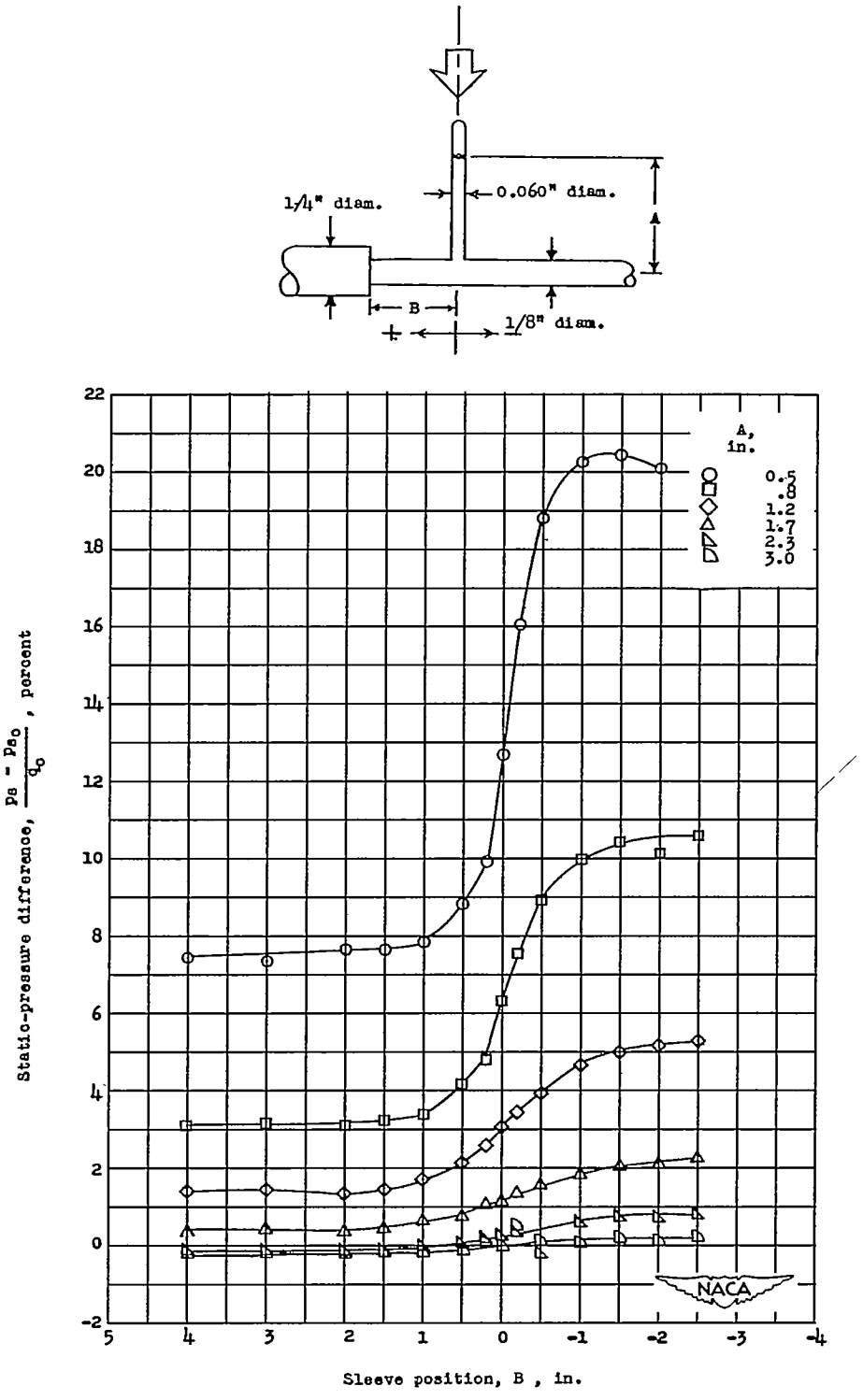

Figure 17.- Difference in static-pressure reading between six test probes and longitudinal probe with sleeve position. Flow velocity, 295 feet per second.

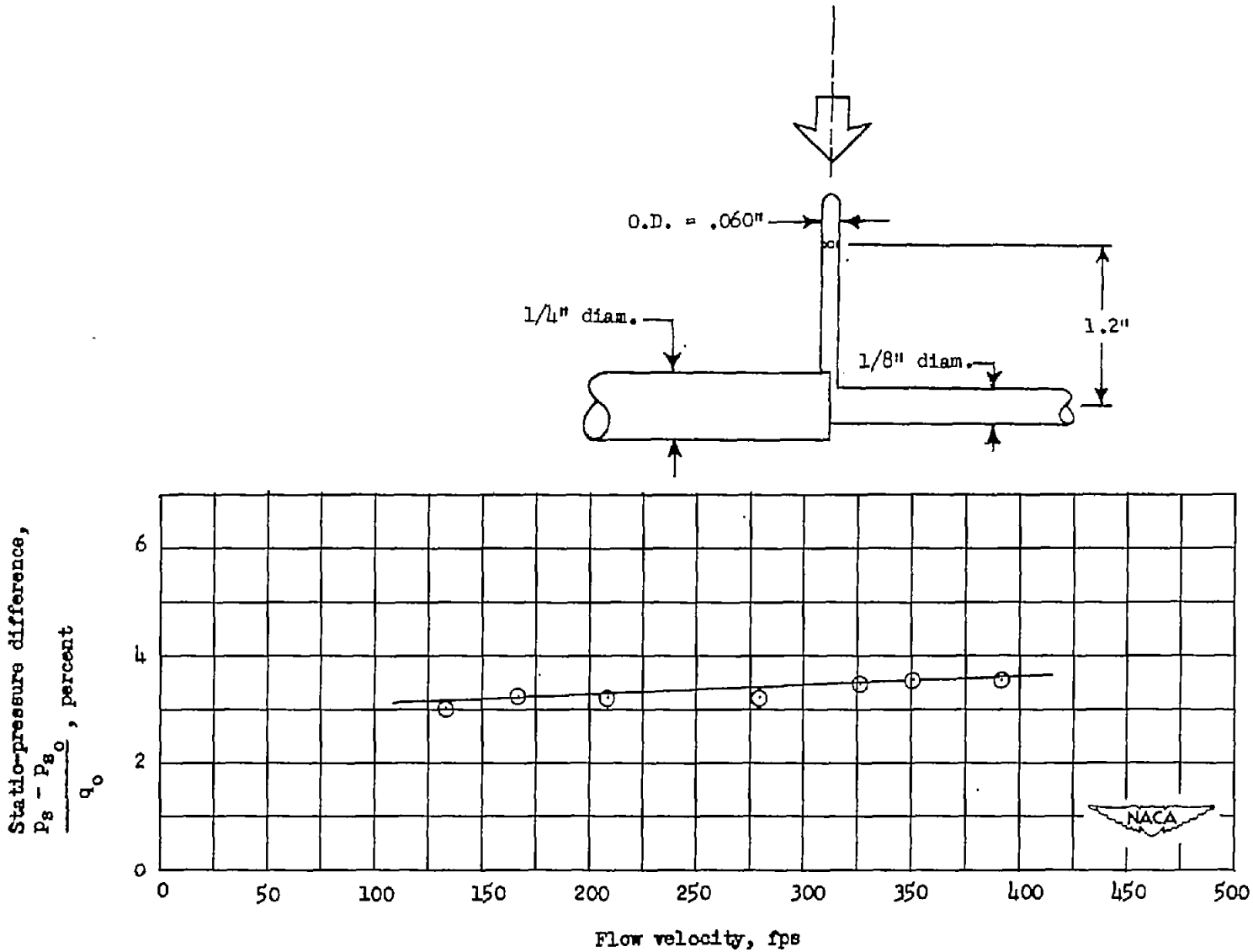

Figure 18.- Difference in static-pressure reading between test probe and longitudinal probe with flow velocity for a typical static probe and sleeve configuration.

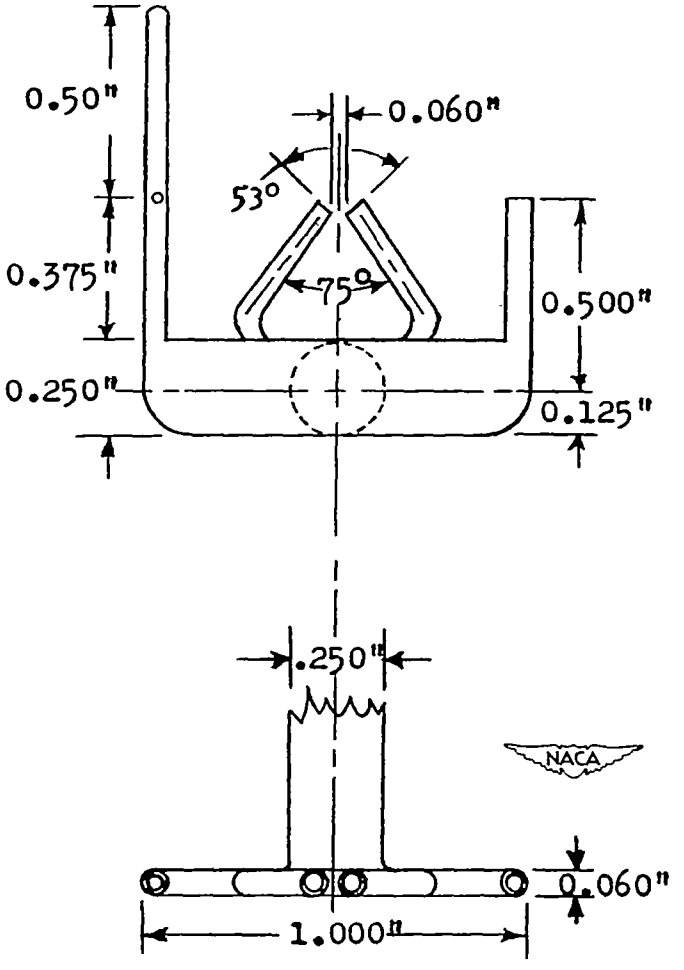

Figure 19.- Details of combination probe type A.

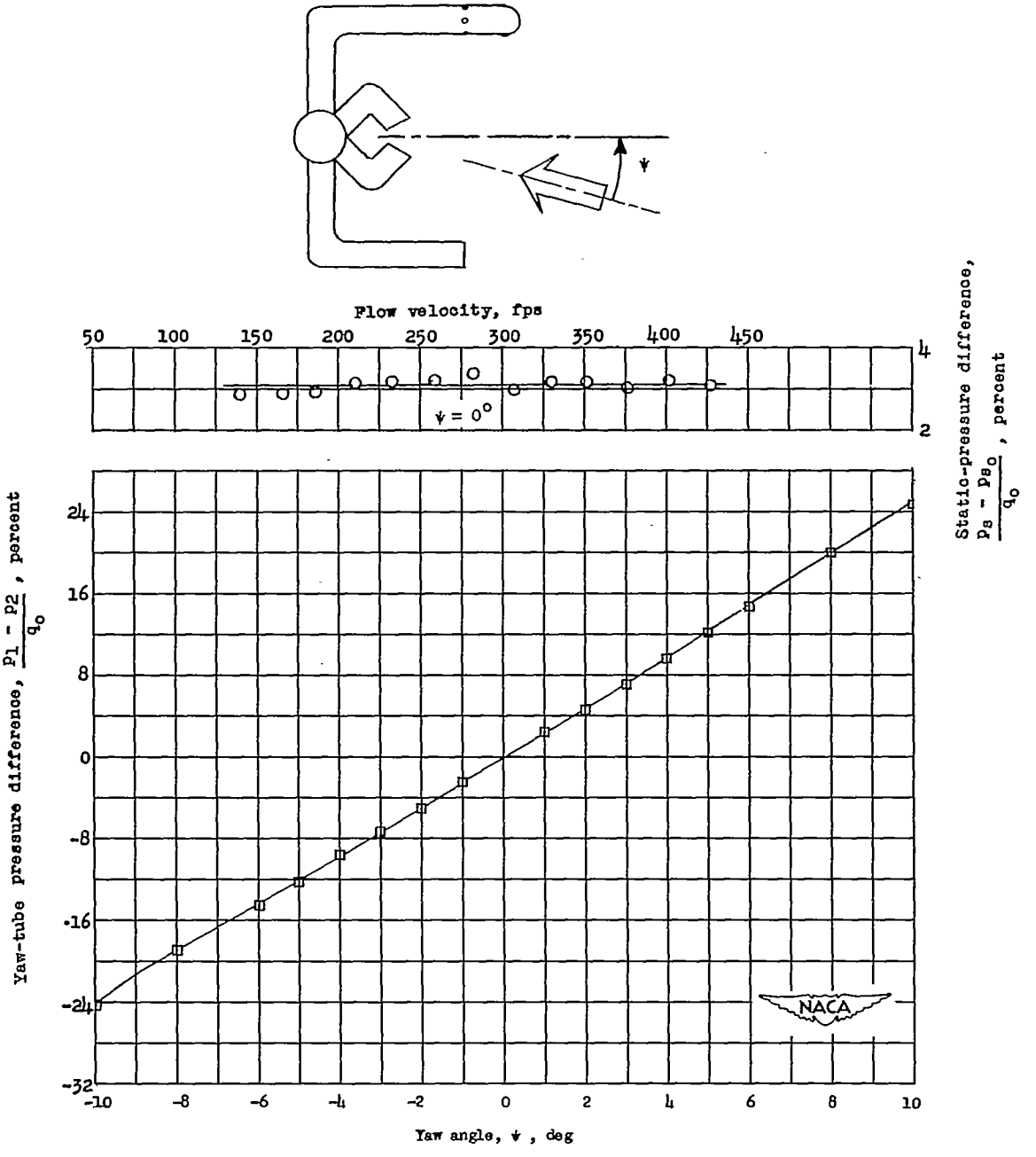

Figure 20.- Variation of yaw-tube pressure difference with yaw angle for flow velocity of 285 feet per second and difference in static pressure reading between probe type A and standard static probe with flow velocity.

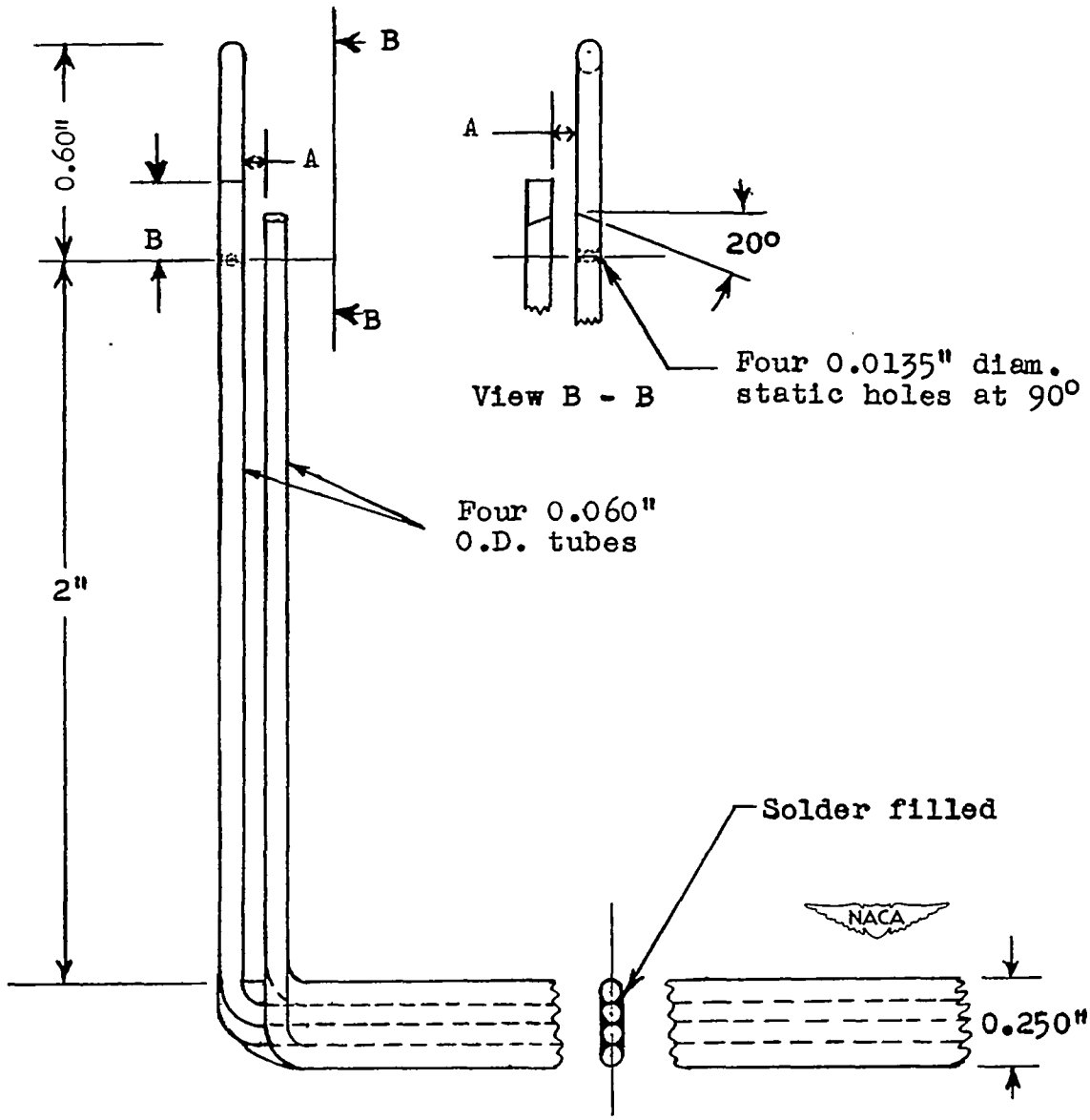

Figure 21.- Details of the type B probe.

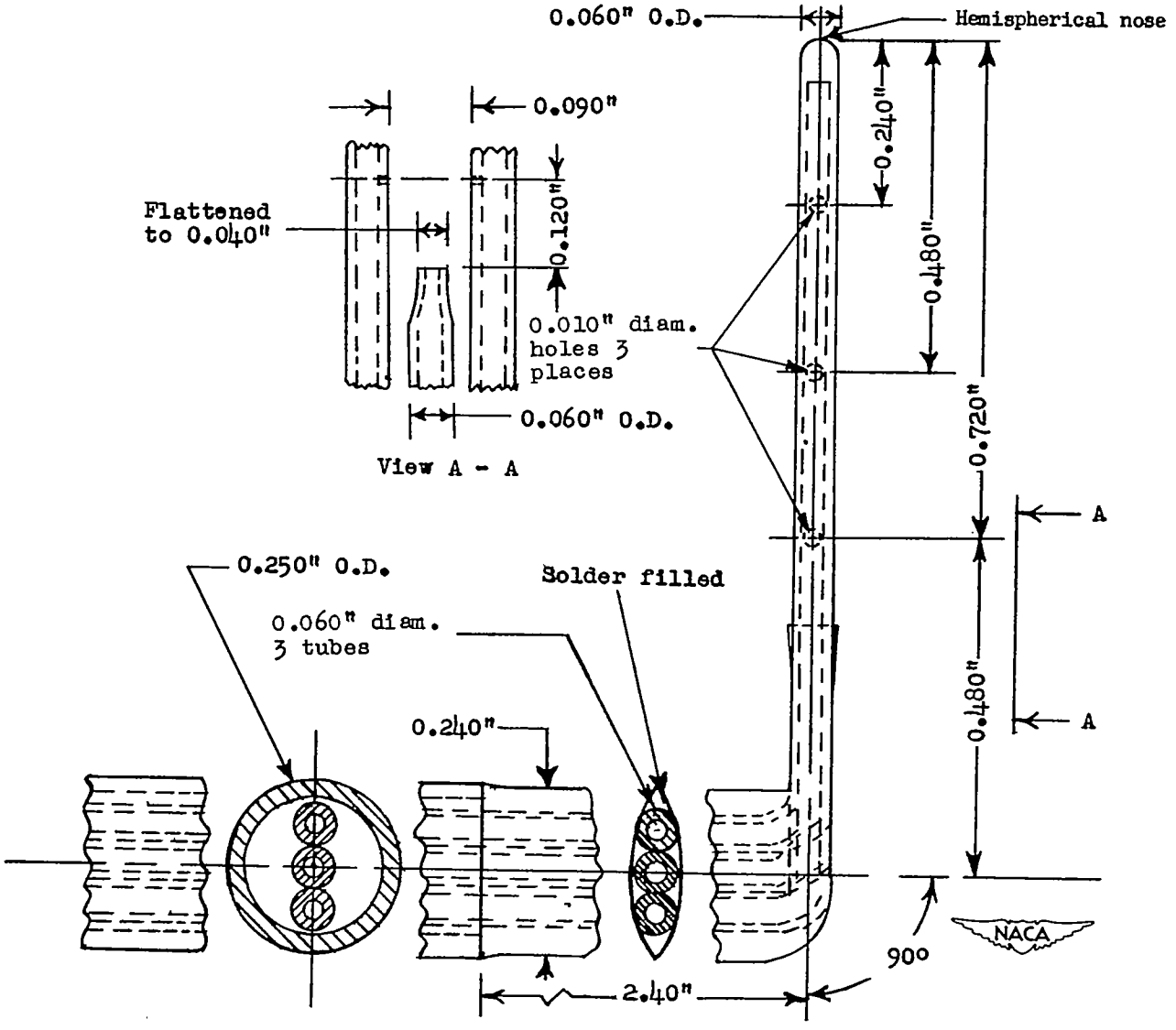

Figure 22.- Details of the combination probe type C.

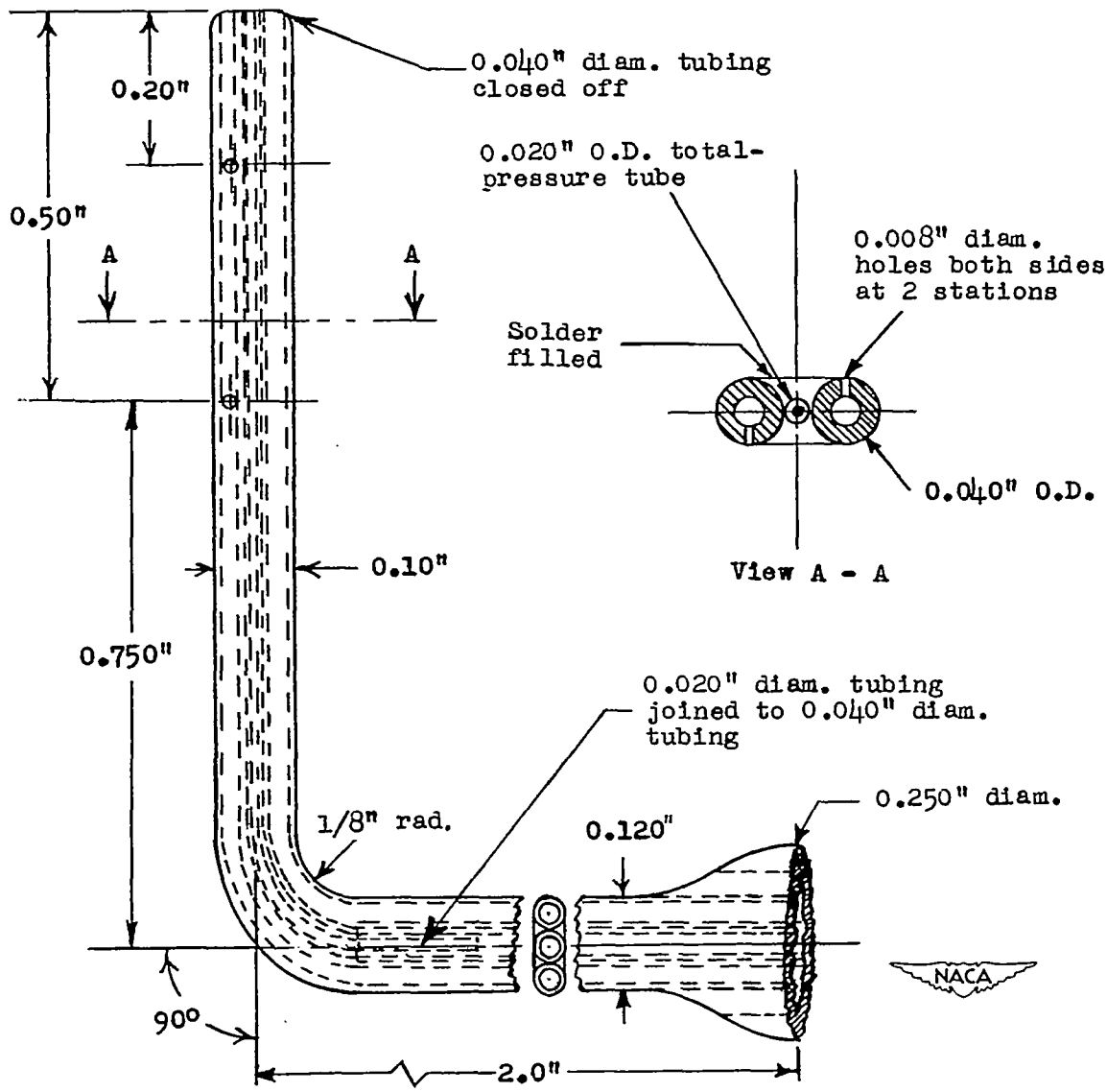

Figure 23.- Details of the combination probe type D.

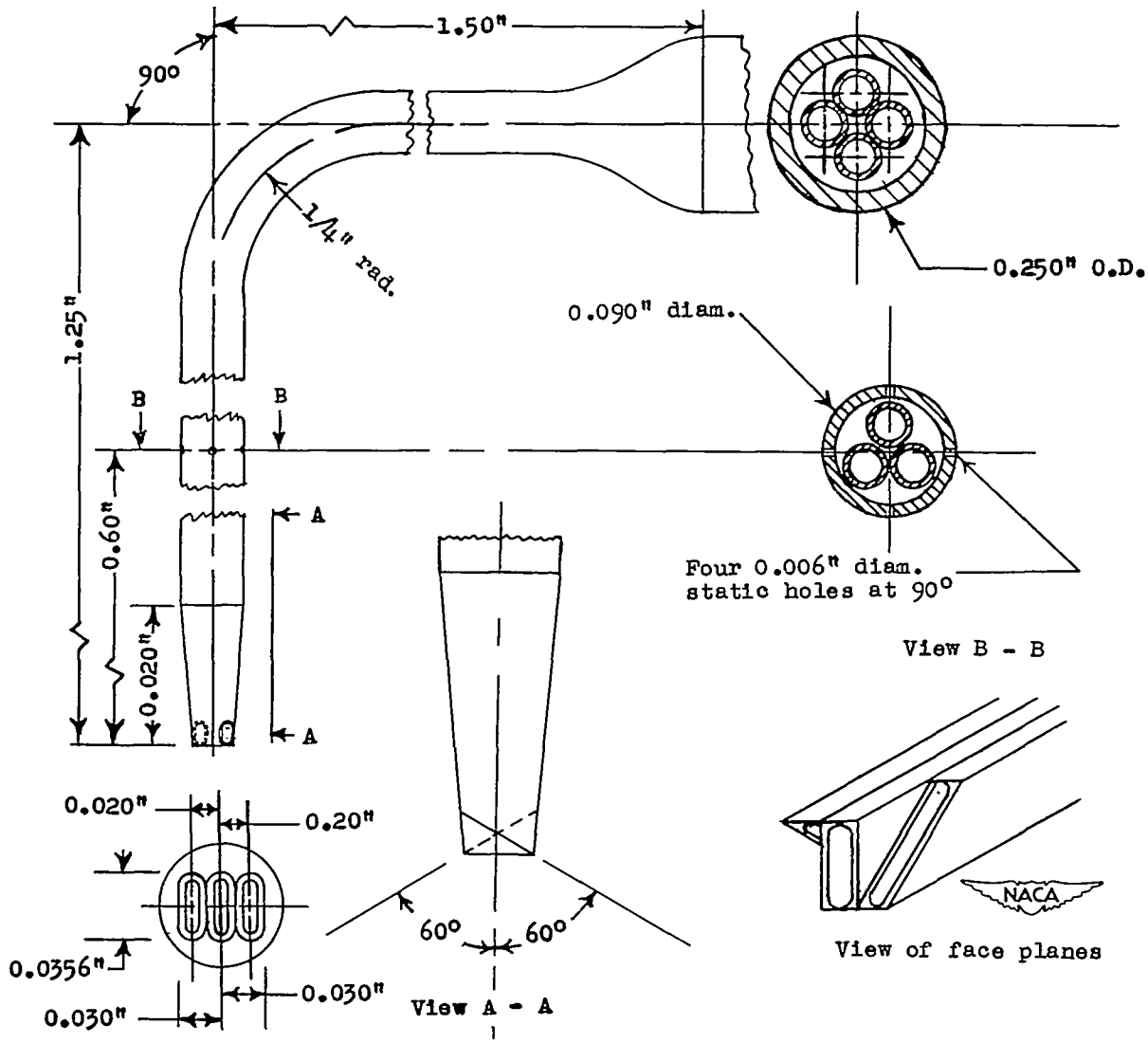

Figure 24.- Details of combination probe type E.

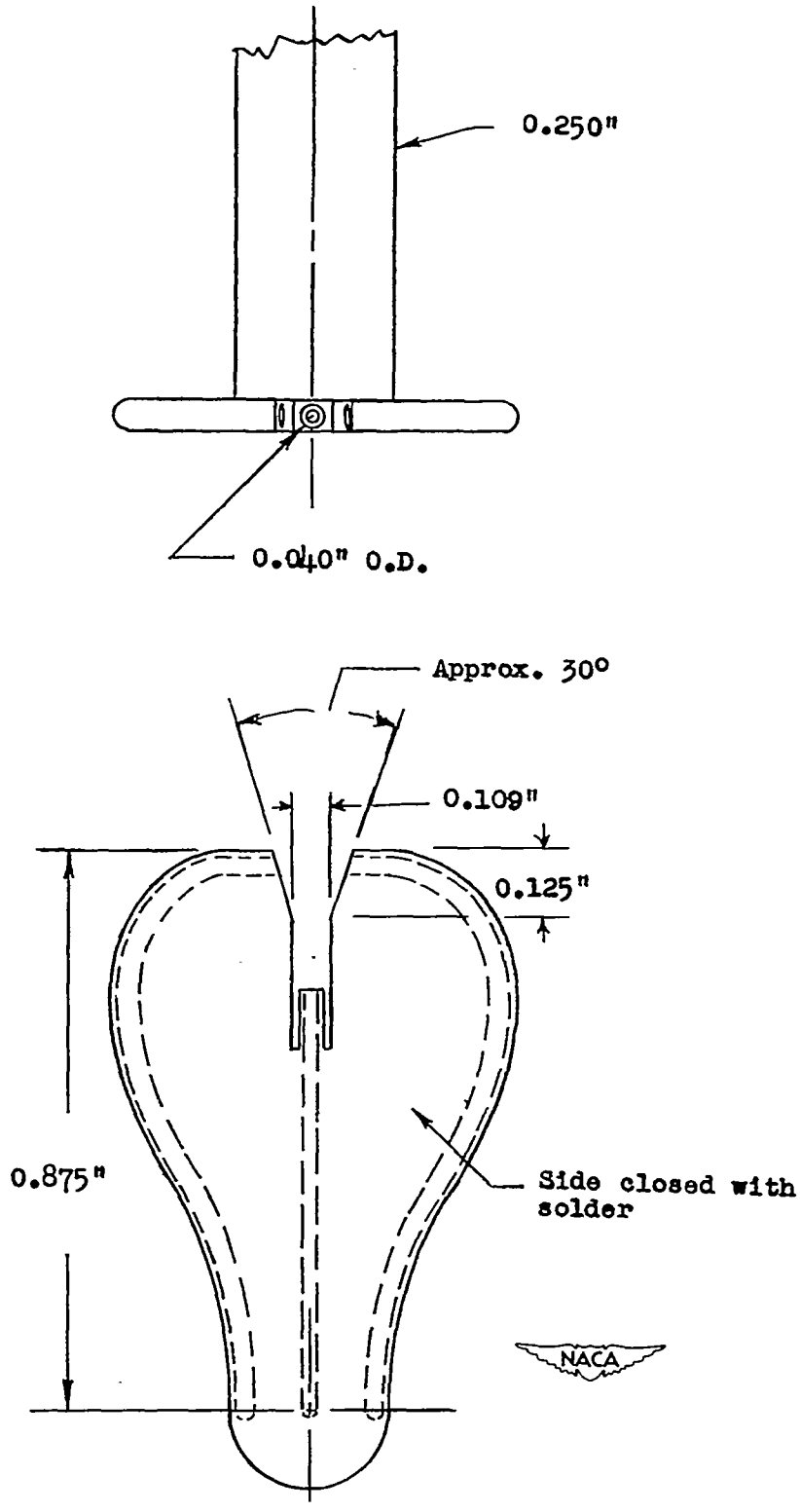

Figure 25.- Details of the combination probe type F.

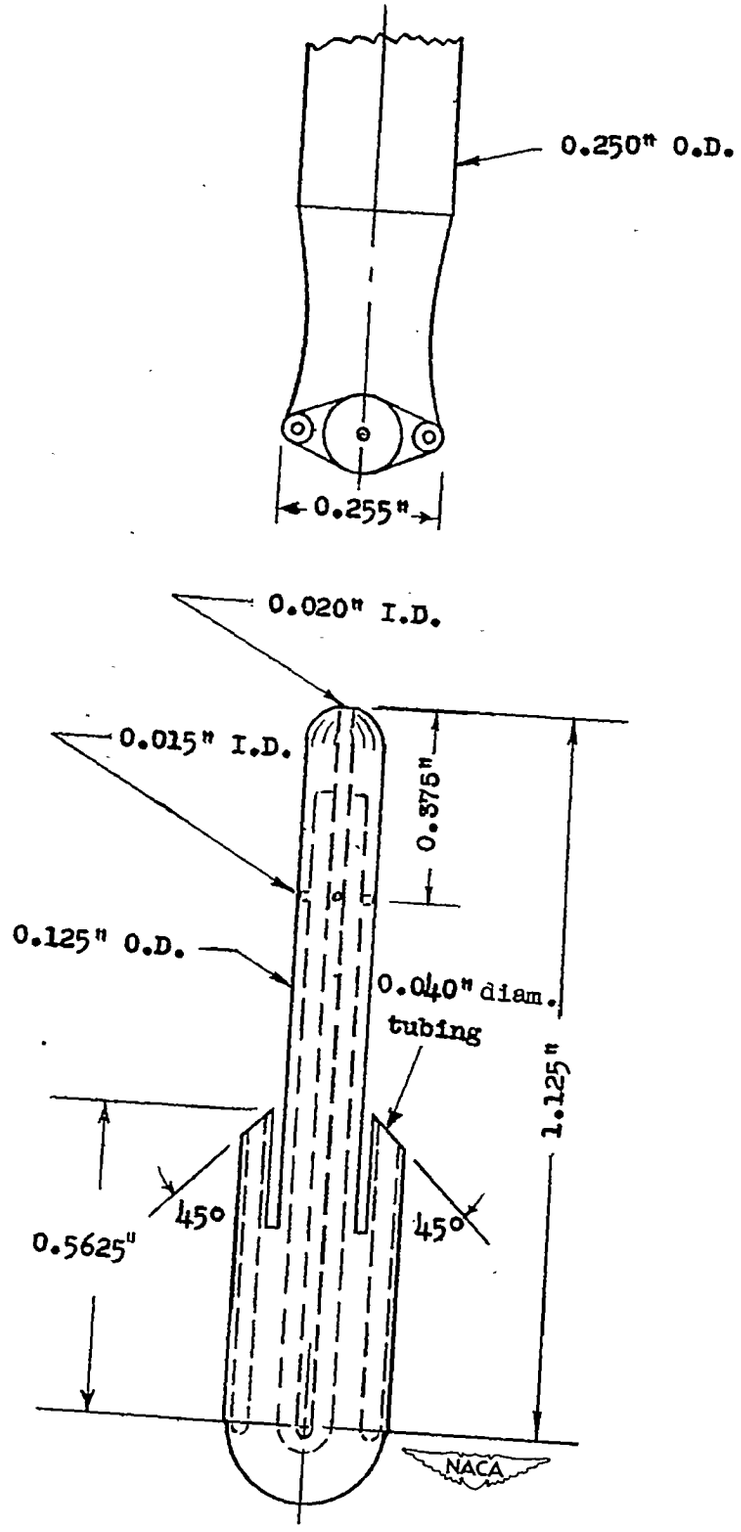

Figure 26.- Details of the combination probe type G.

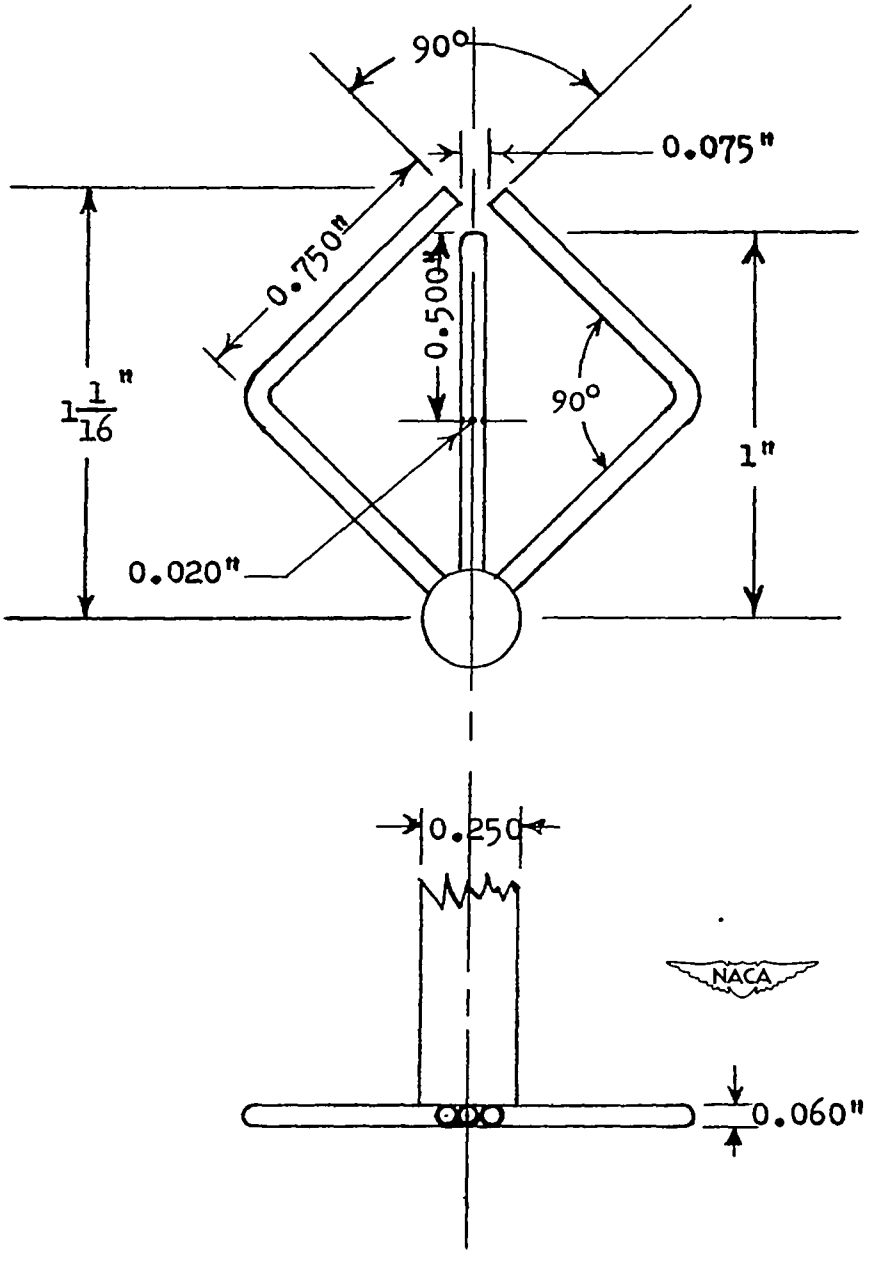

Figure 27.- Details of the combination probe type H.

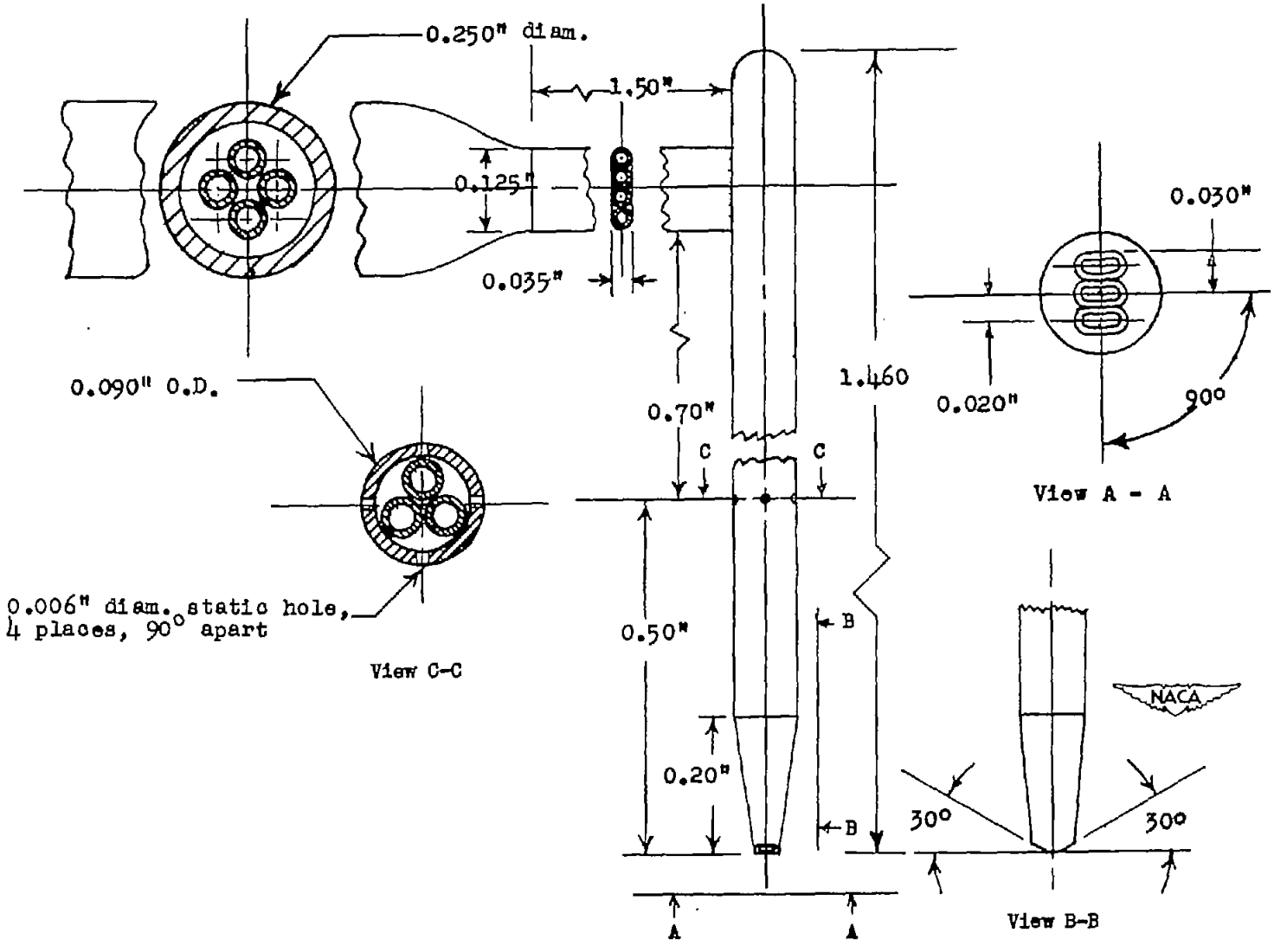

Figure 28.- Details of prism-type combination probe.

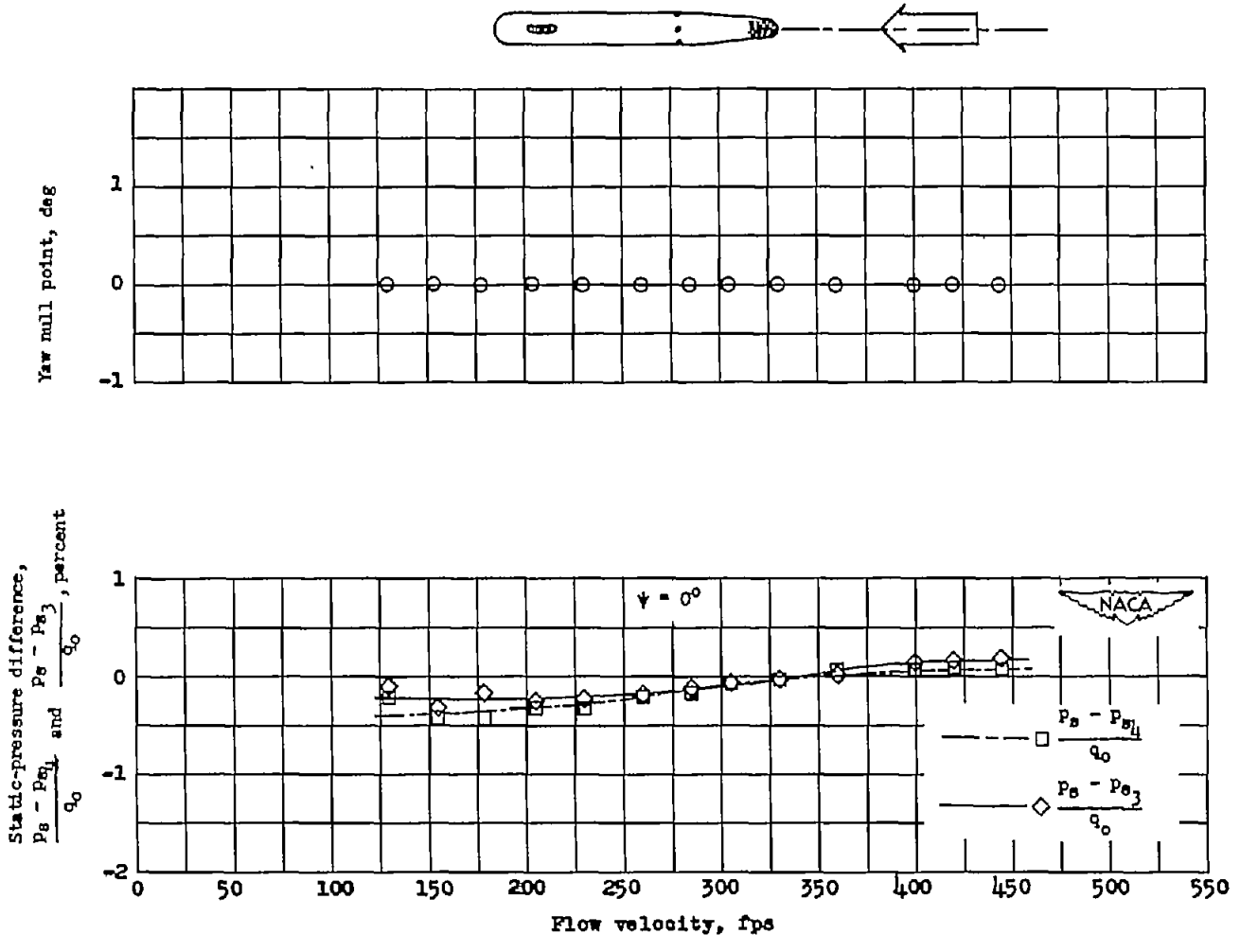

Figure 29.- Variation of yaw null point and difference in static-pressure reading between the prism-type probe and longitudinal probe and between the prism-type and standard probe with flow velocity.

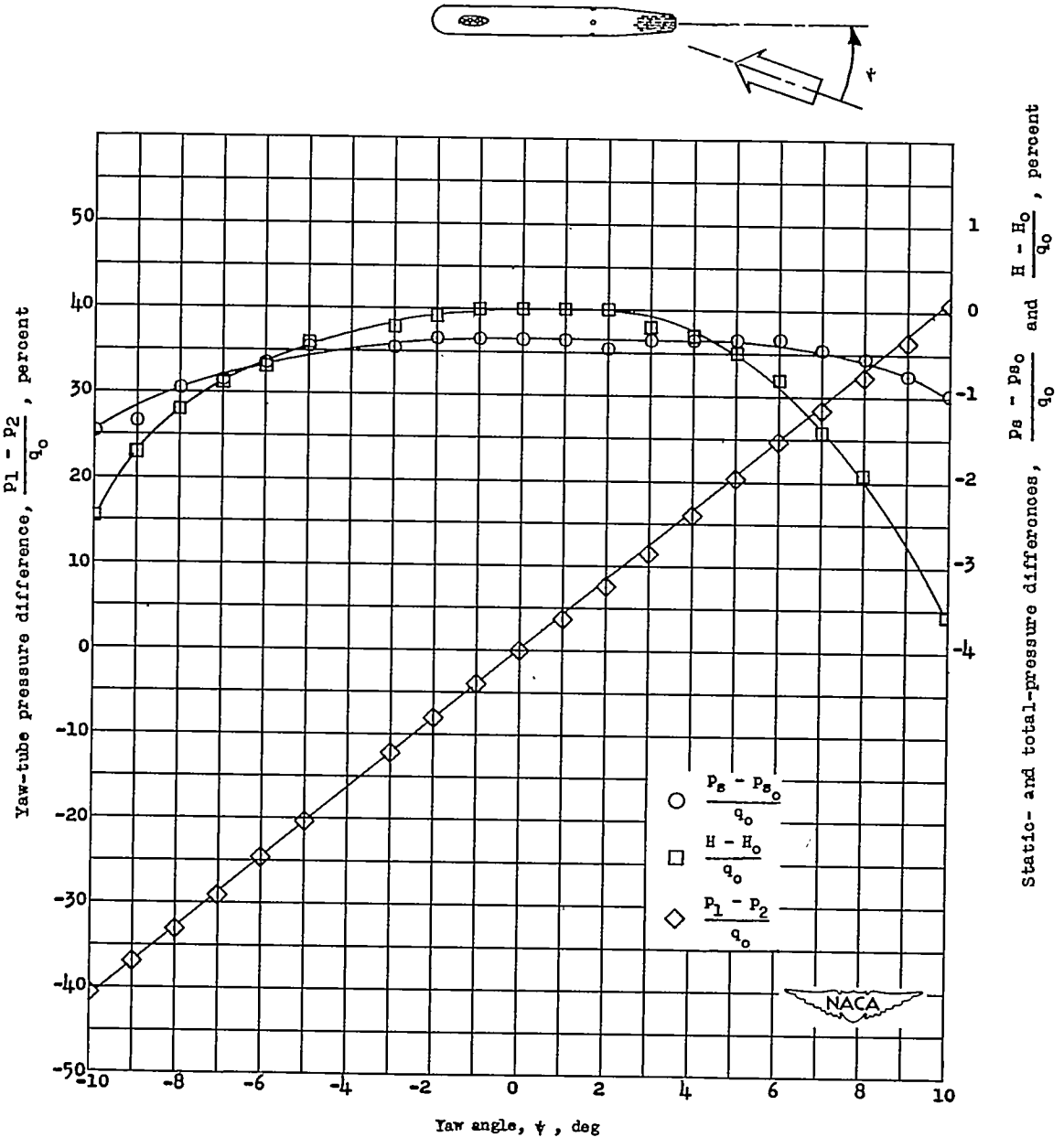

(a) Flow velocity, 197 feet per second.

Figure 30.- Variation of yaw-tube pressure difference and differences in static- and total-pressure readings between the prism-type probe and standard static- and total-pressure probes with yaw angle.

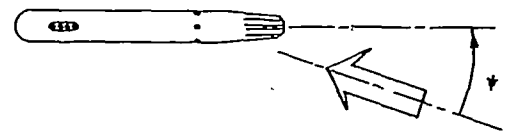

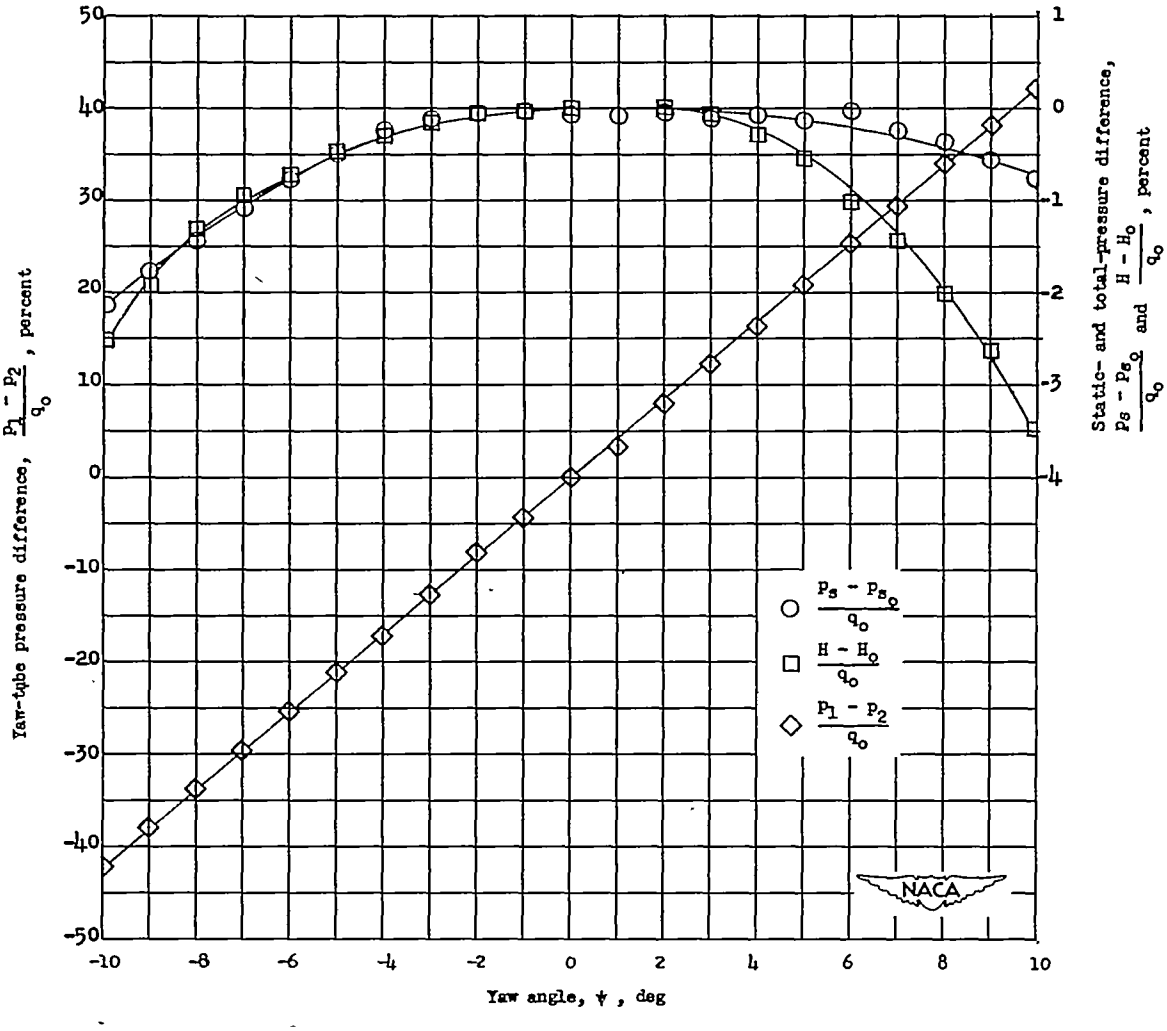

(b) Flow velocity, 390 feet per second.

Figure 30.- Concluded.

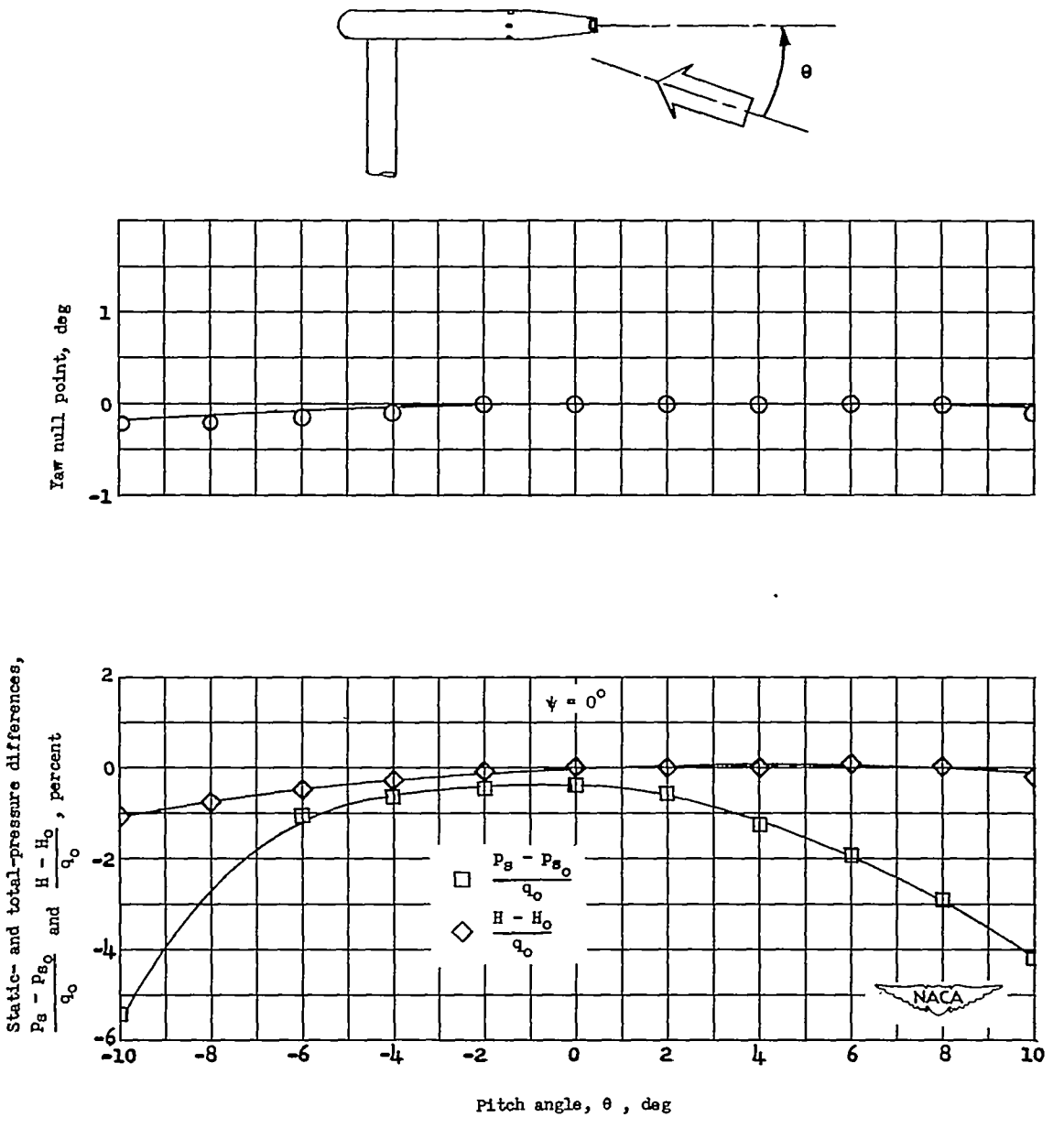

(a) Flow velocity, 196 feet per second.

Figure 31.- Variation of yaw null point and differences in static- and total-pressure readings between prism-type probe and standard static- and total-pressure probes with pitch angle.

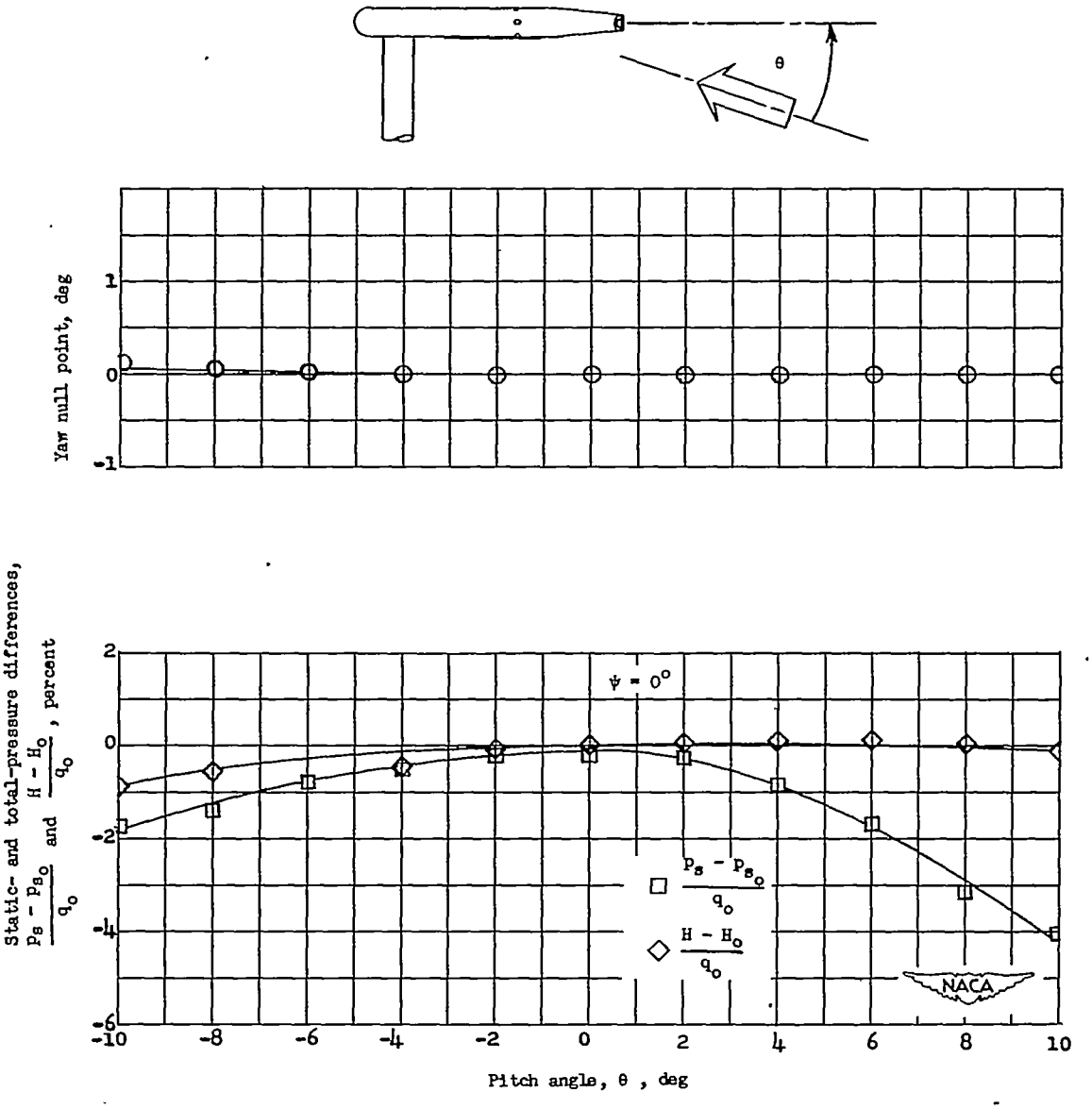

(b) Flow velocity, 308 feet per second.

Figure 31.- Concluded.

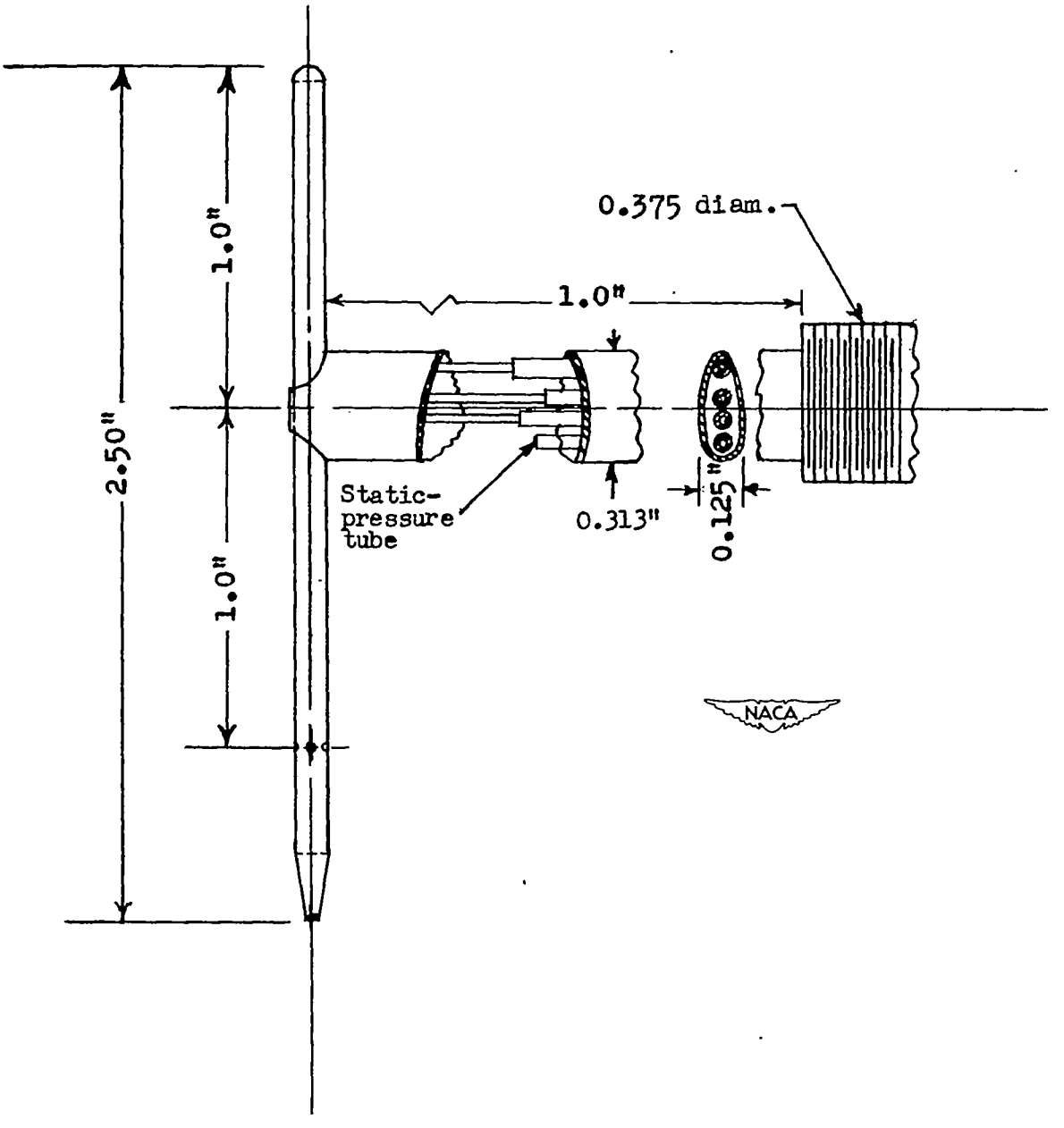

Figure 32.- Details of prism-type combination probe designed for mounting on a rotor.

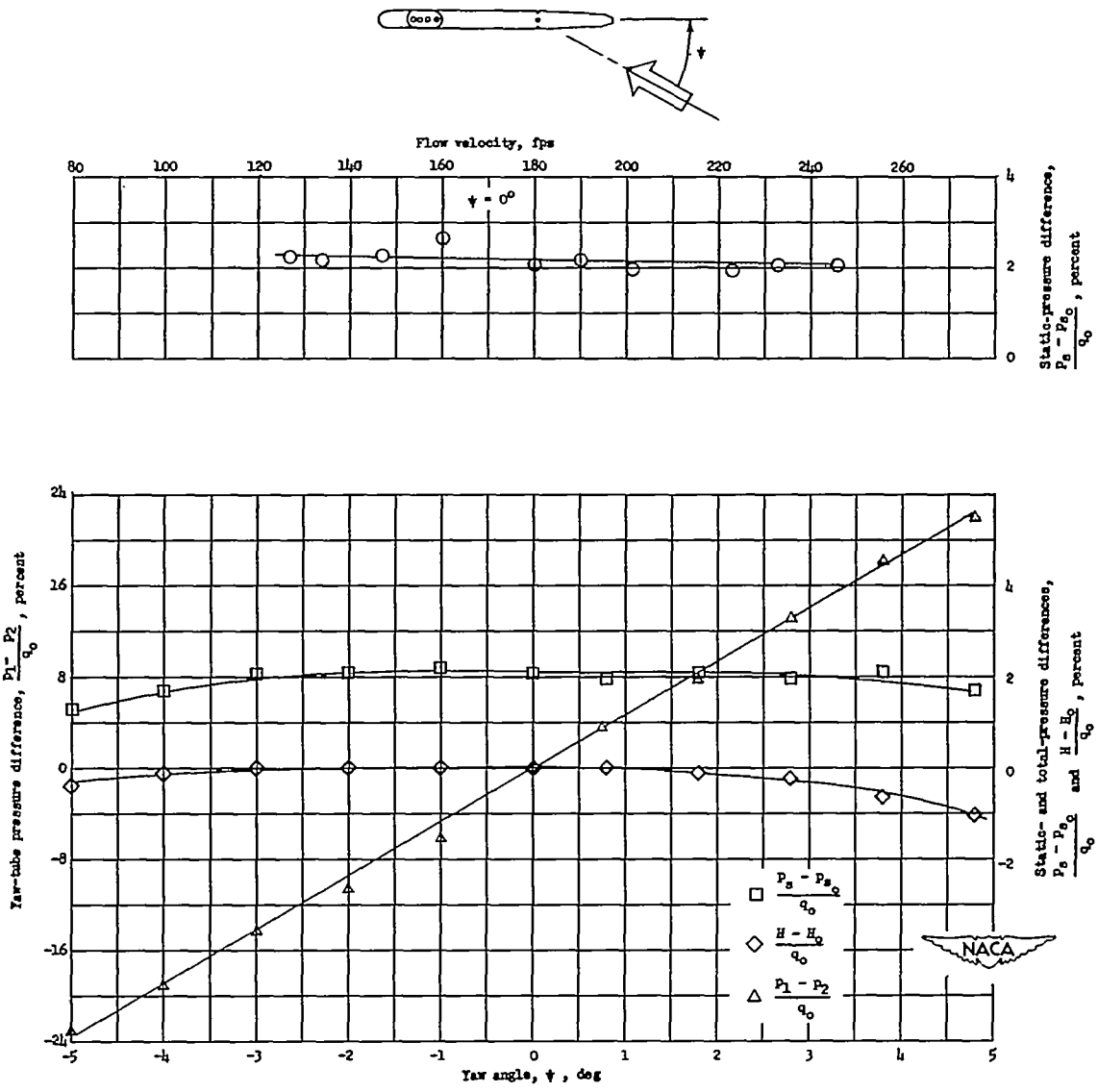

Figure 33.- Variation of yaw-tube pressure difference and differences in static- and total-pressure readings at 155 feet per second with yaw angle and variation of difference in static-pressure reading with flow velocity between the prism-type probe designed for mounting on a rotor and standard static- and total-pressure probes.

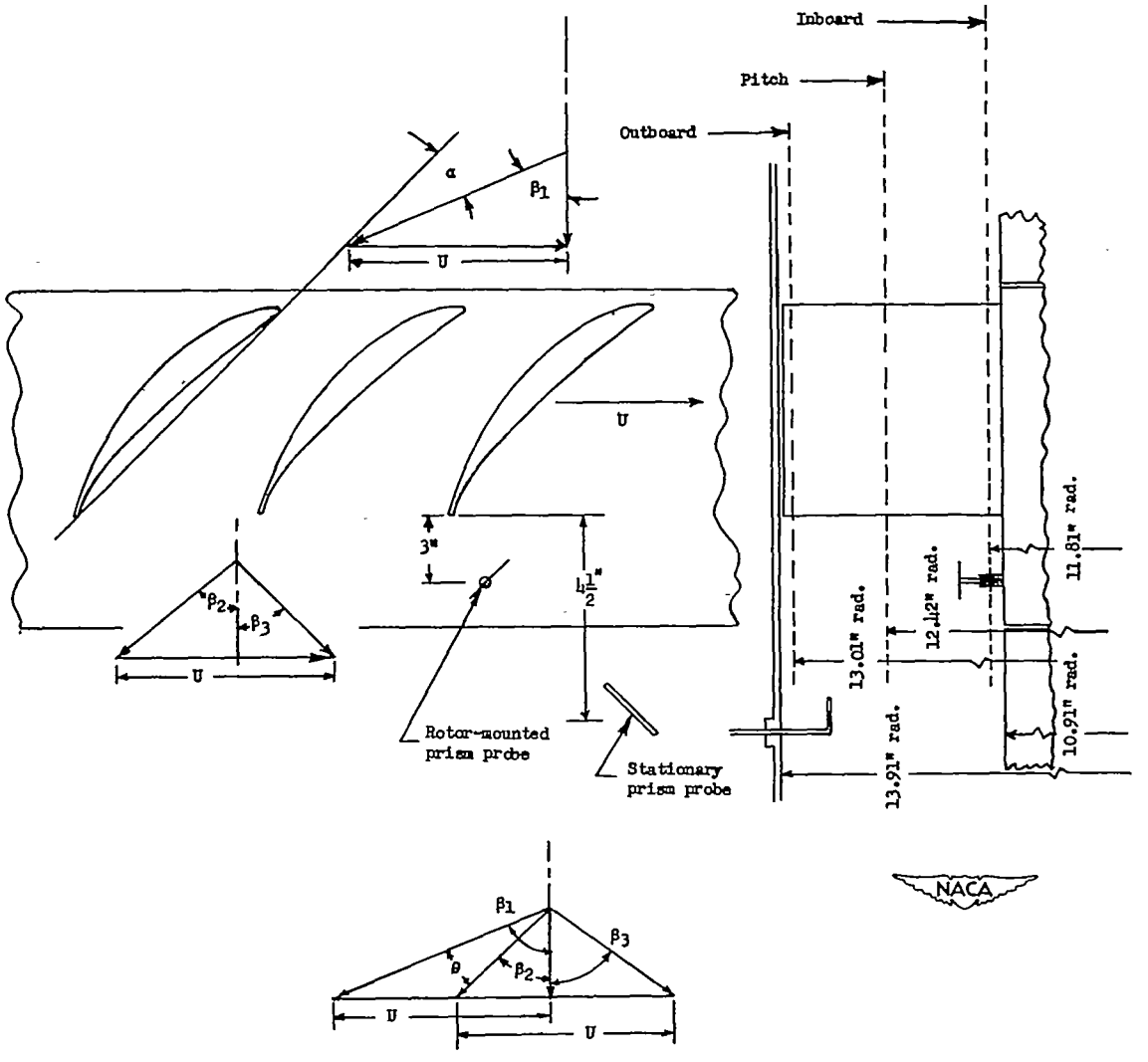

β_1 air inlet angle relative to rotor, deg

β_2 air exit angle relative to rotor as read by rotor-mounted probe, deg

β_3 air exit angle relative to stator as read by stationary probe, deg

θ turning angle, $\beta_1 - \beta_2$, deg

α angle between chord and entering air, deg

U rotor velocity, fps

Figure 34.- Sketch showing setup used in the rotor-mounted-probe test. Not to scale.

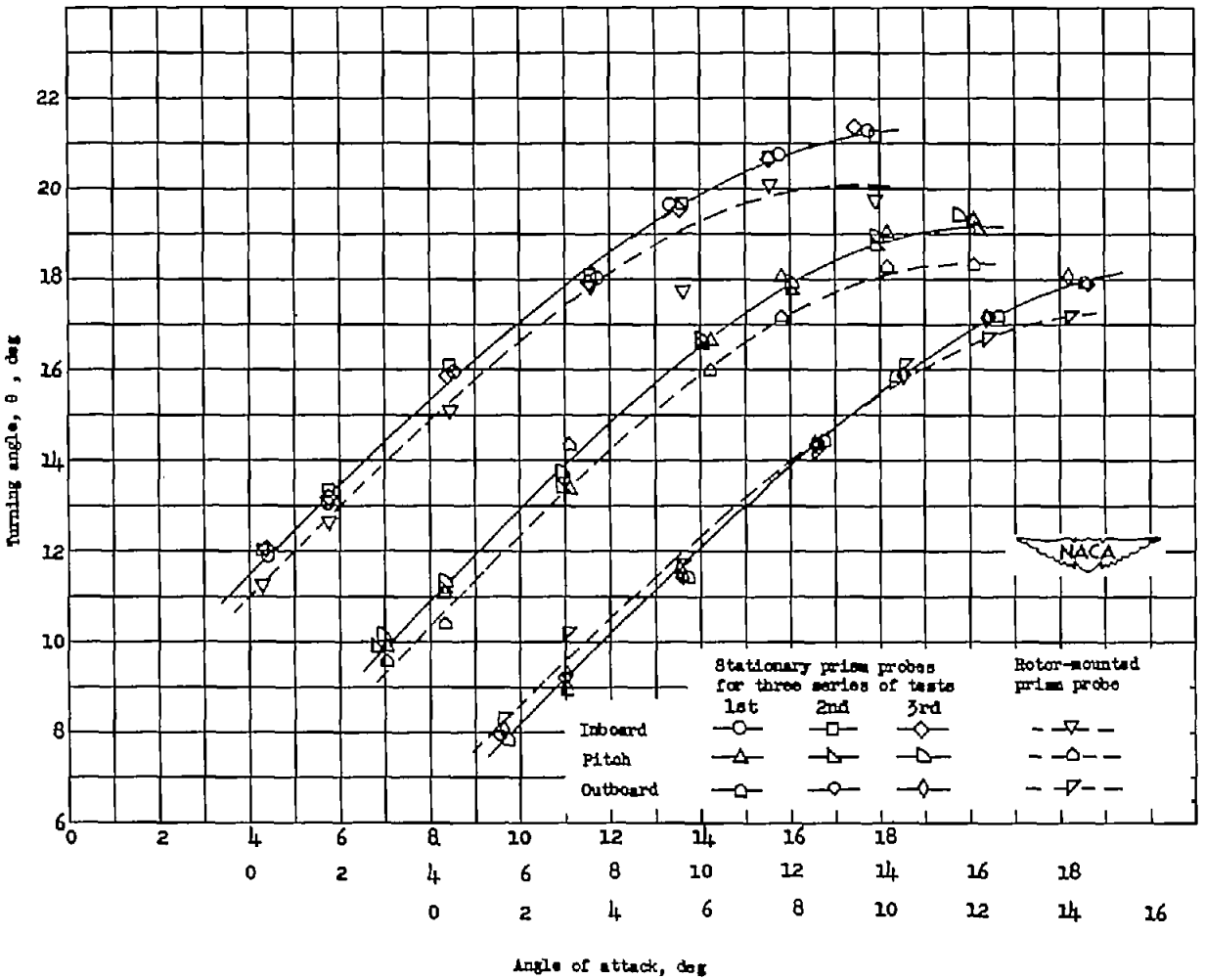

Figure 35.- Comparison of flow angles at three radii of a compressor rotor as measured by both stationary and rotor-mounted prism probes. Flow velocity, 154 to 194 feet per second.

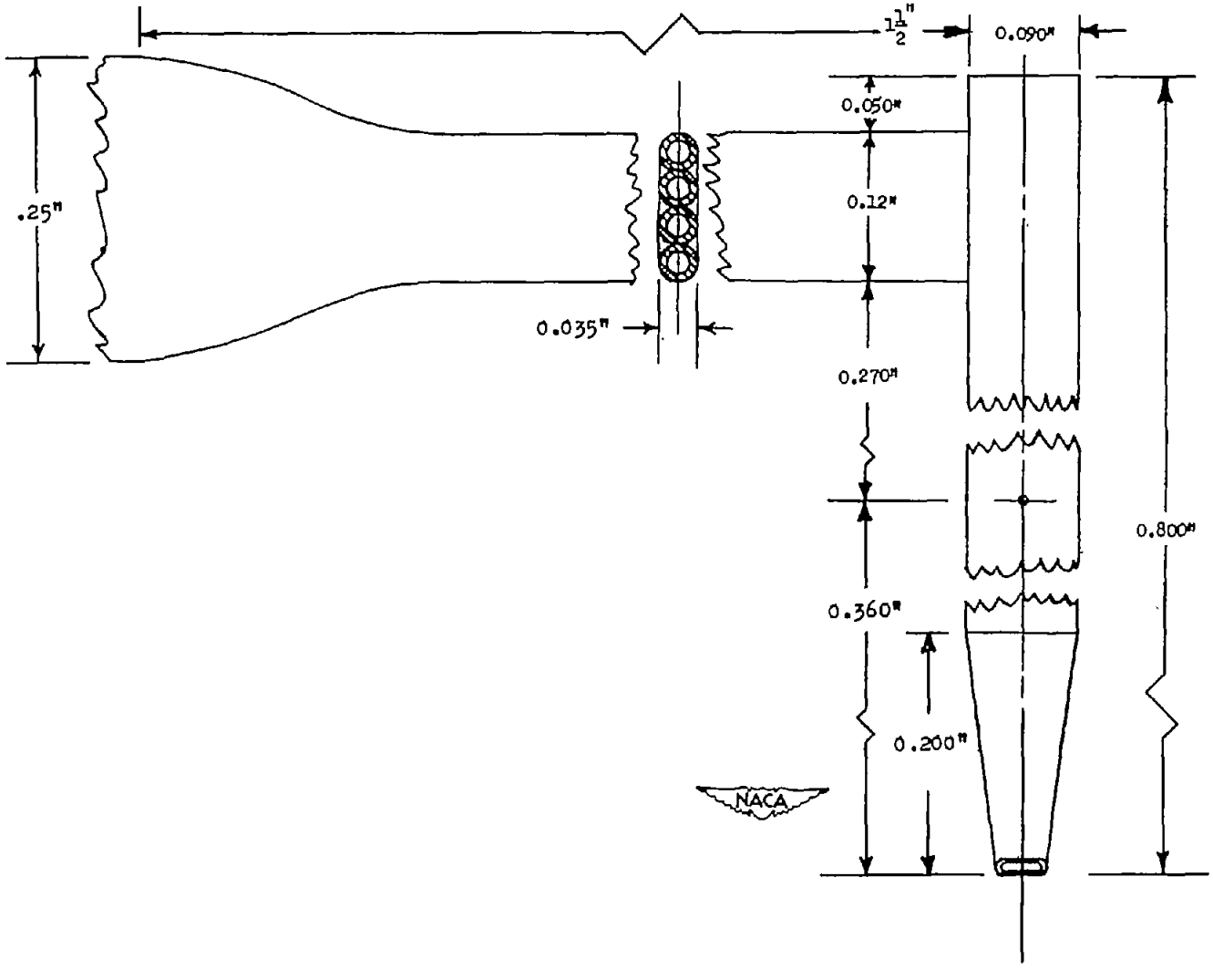

Figure 36.- Detail of the short prism-type probe.

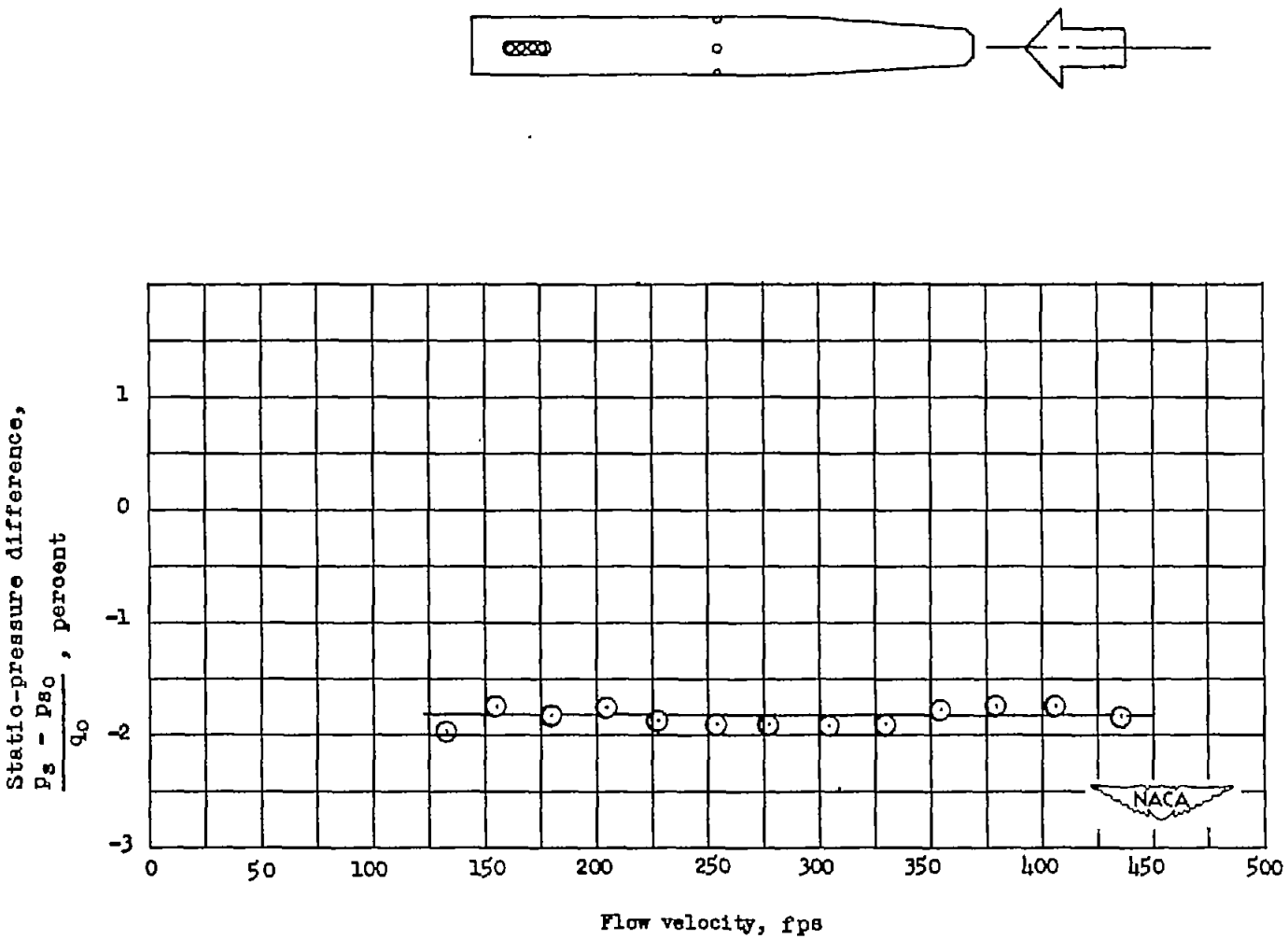

Figure 37.- Variation of the difference in static-pressure reading between the short prism-type probe and the longitudinal probe with flow velocity. $\psi = 0^{\circ}$.

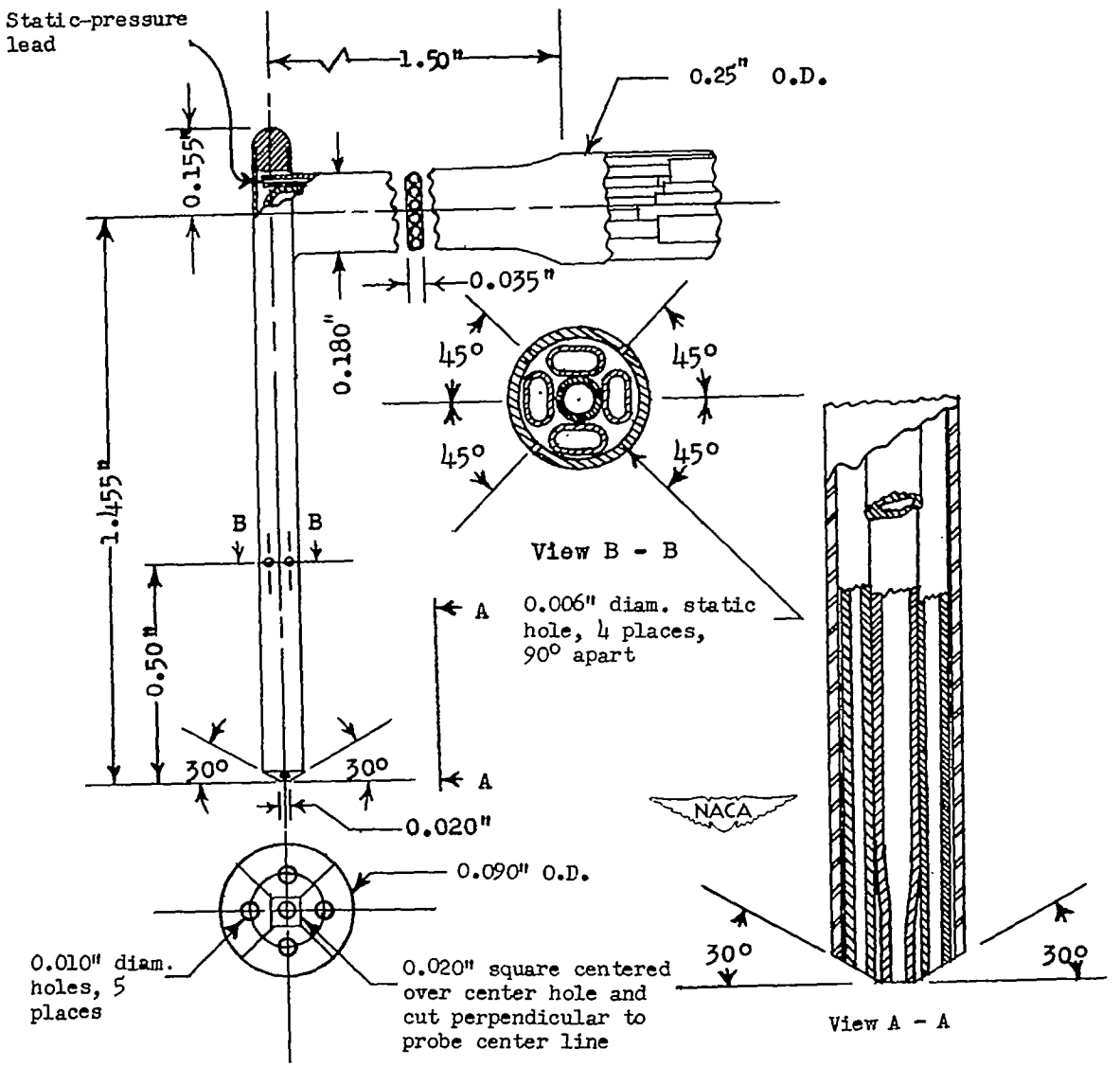

Figure 38.- Details of pyramid-type combination probe.

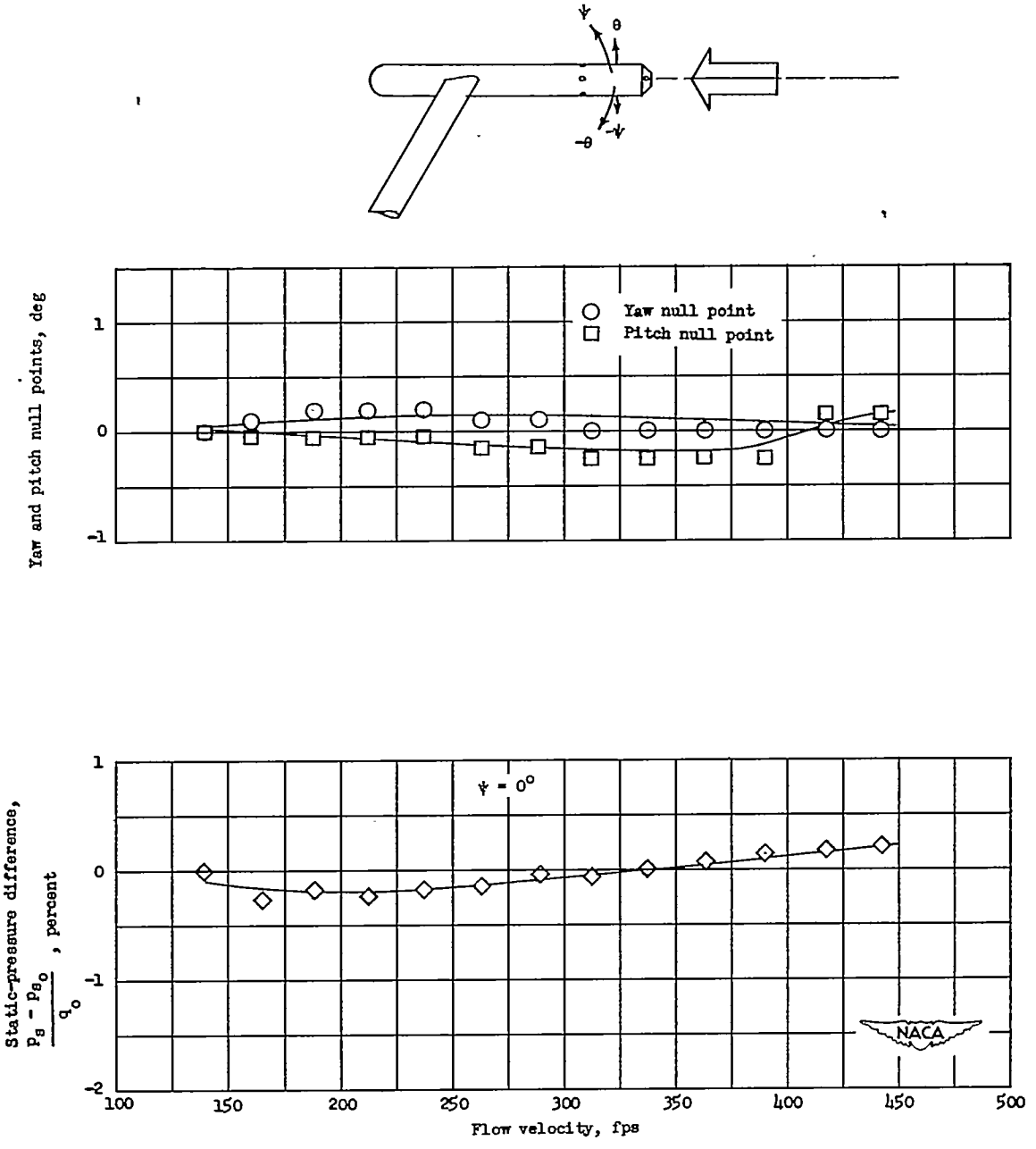

Figure 39.- Variation of yaw and pitch null points referred to a value at flow velocity of 139 feet per second and difference in static-pressure reading between the pyramid-type probe and the longitudinal probe with flow velocity.

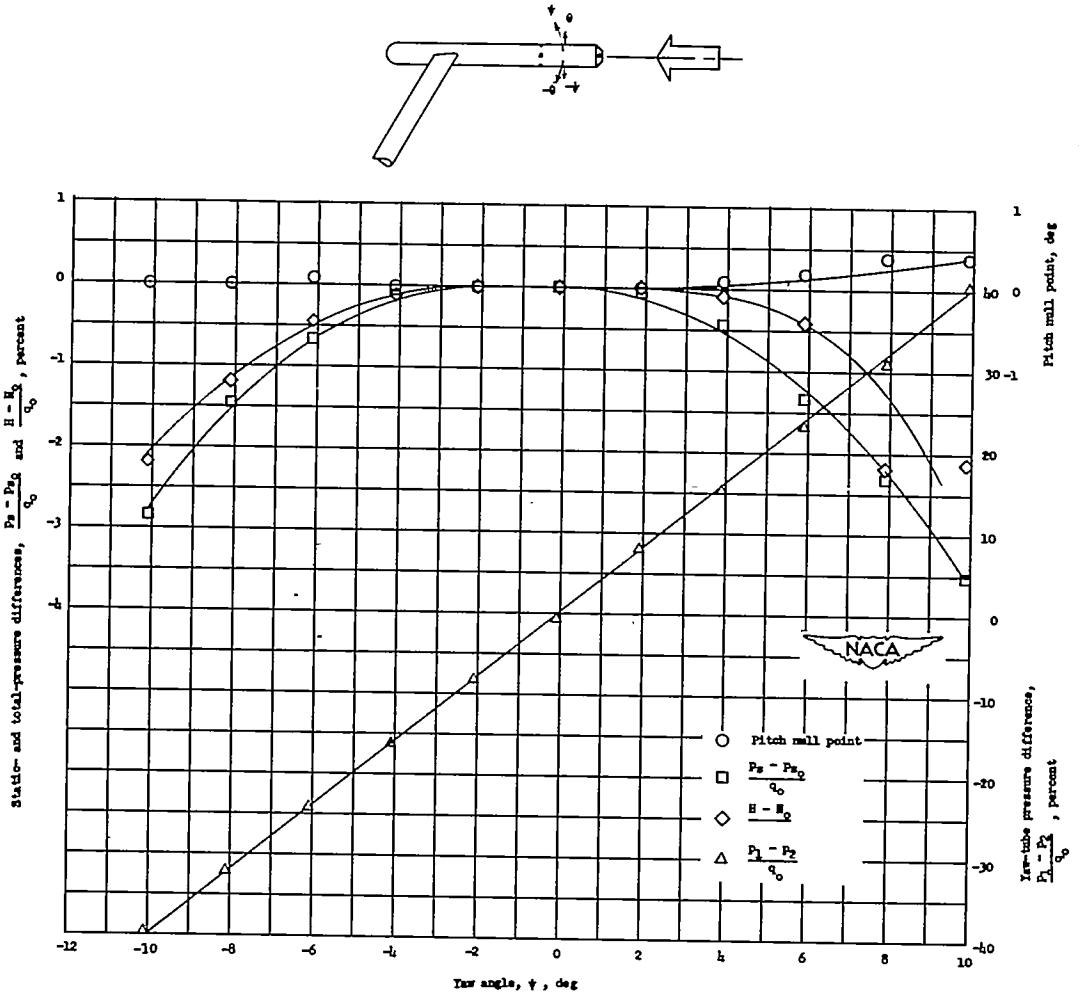

Figure 40.- Variation of pitch null point, yaw-tube pressure difference, and difference in static- and total-pressure readings between pyramid-type probe and longitudinal and standard total-pressure probes with yaw angle. Flow velocity, 402 feet per second.

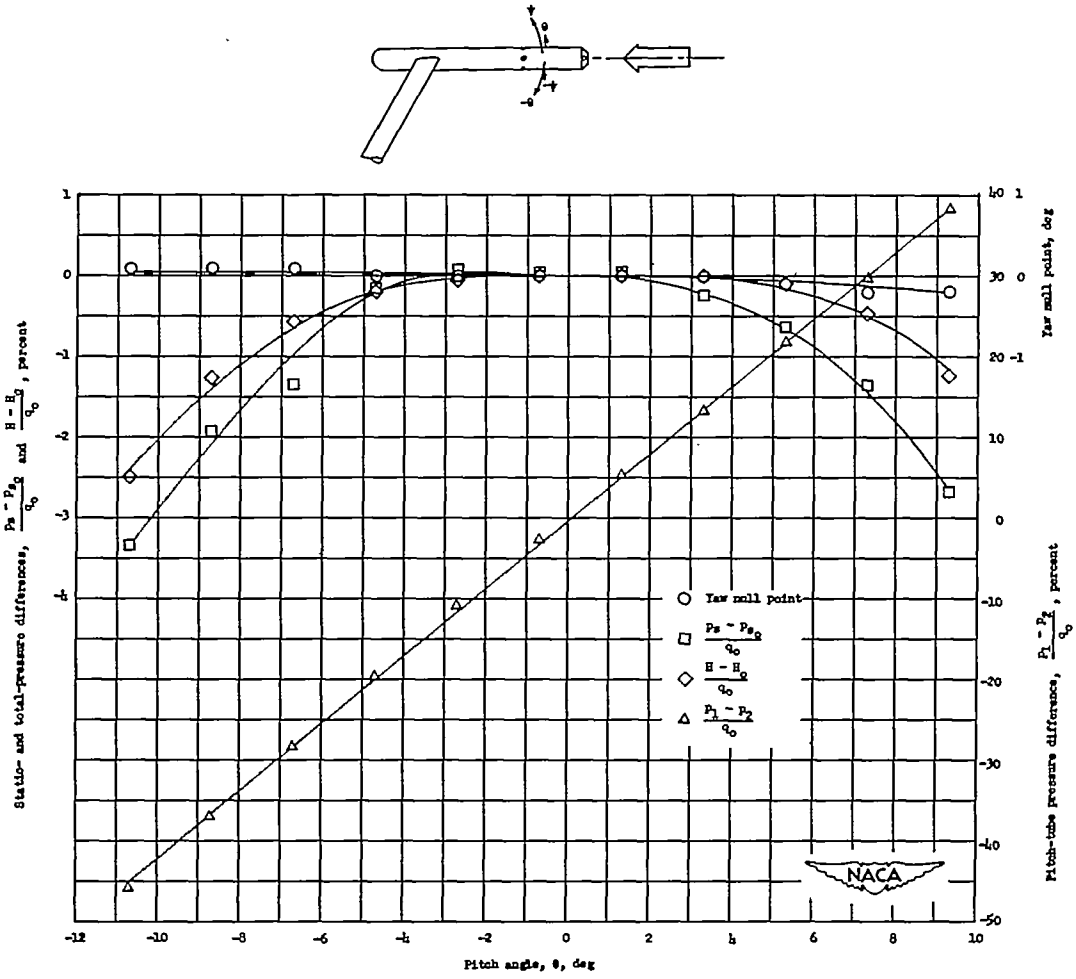

Figure 41.- Variation of pitch-tube pressure difference, yaw null point, and difference in static- and total-pressure readings between pyramid-type probe and longitudinal probe and standard total-pressure probe with pitch angle. Flow velocity, 402 feet per second.

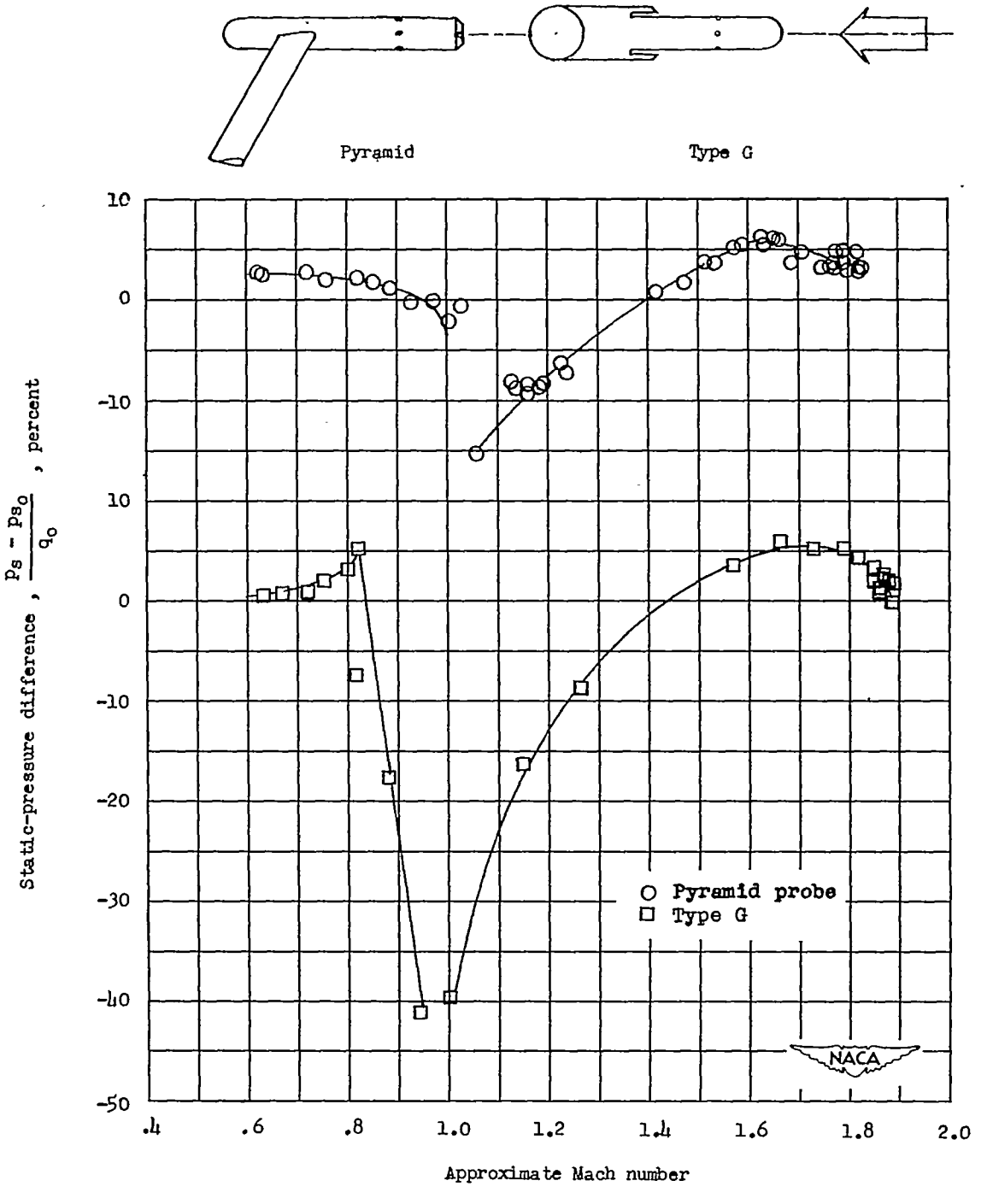

Figure 42.- Variation of the difference in static-pressure readings between the pyramid probe and a standard probe and between survey probe G and a standard probe in a Freon-12 atmosphere with approximate Mach number. $\psi = 0^{\circ}$.

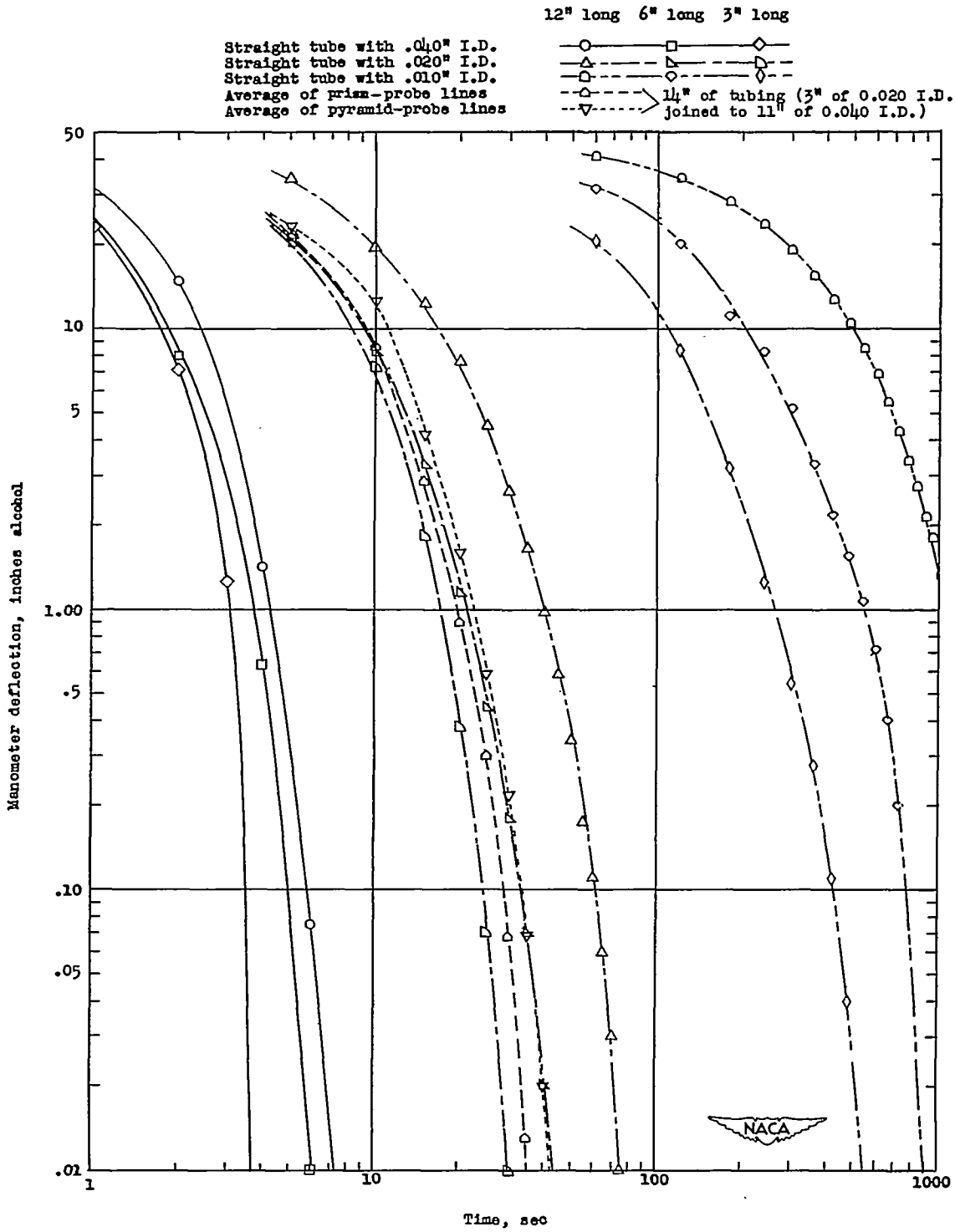

Figure 43.- Variation of manometer-tube (0.156 in. I.D.) deflection with time for various size tubes as compared to the prism- and pyramid-probe reaction characteristics.

NACA-Langley - 2-18-54 - 75